Chapter 19

Air–Water Exchange

Environmental Organic Chemistry, Third Edition. René P. Schwarzenbach, Philip M. Gschwend, and Dieter M. Imboden.
Copyright © 2017 John Wiley & Sons, Inc. Published 2017 by John Wiley & Sons, Inc.
Companion website: www.wiley.com/go/Schwarzenbach/EnvironmentalOrganChem3e

19.1 The Air–Water Interface

Air and water are the two most important fluids on earth (see Chapter 5). The atmosphere and the hydrosphere are complementary in their roles of transporting and transforming chemicals. The atmosphere is the fastest and most efficient global conveyor belt. However, because of their physicochemical properties, certain chemicals prefer aquatic *milieu*. Since air–water exchange closely couples the two fluid systems, chemicals can appear in aquatic systems far away from their sources at times much shorter than needed for transport in purely aqueous aquatic systems.

The size of the interface between atmosphere and hydrosphere is immense. A large area of the Earth's surface (361×10^6 km^2, 71%) is covered by water (Table 5.1) whose surface is in contact with the atmosphere. In addition, the atmosphere contains about 25 kg m^{-2} of water (Stevens and Bony, 2013). Most of it is present as water vapor, but about 0.5% is in liquid form (around 0.1 kg m^{-2}), that is, in cloud droplets with a typical diameter of 10 µm, each having a mass of about 0.5×10^{-12} kg. These droplets (about 2×10^{11} per m^2 of earth surface) have a surface area of about 60 m^2 per m^2 of Earth surface. They form a water–air contact area many times larger than the contact area at the surface of the ocean.

We are often concerned with the transfer of chemicals between gaseous and liquid phases that are not at equilibrium. Such disequilibrium results from the large size of the environmental systems involved since chemicals cannot be quickly transferred from the system's interior to the exterior and then into the adjacent phases. In these systems, natural biogeochemical reactions as well as processes associated with human endeavors including spilling of chemicals into the environment are continuously driving the global systems away from equilibrium. Also, partition coefficients such as the Henry's law coefficient (Chapter 9) depend on temperature, which of course varies with space and time, so adjacent air and water systems are also continuously pushed out of equilibrium.

The physical processes at the surfaces of oceans, estuaries, rivers, and lakes that are relevant to the exchange of chemicals are extremely complicated and variable. We are not always able to clearly classify such air–water interfaces as a "bottleneck boundary" or a "wall boundary" (Chapter 18). Therefore, for a quantitative description of chemical fluxes at these important environmental interfaces, we have to make use of a mixture of theoretical concepts and empirical knowledge. Fortunately, this combination is often sufficient to allow reasonable predictions of the rates of chemical exchanges without knowing the exact nature of the exchange process.

We derived all the necessary mathematical tools in Chapters 17 and 18. In essence, whatever the physical nature of the exchange, the flux equation always has the form of a concentration difference times a velocity. In this chapter, compartment 1 and 2 always refers to water (w) and air (a) respectively. From Eq. 18-13, we get:

$$F_{i\mathrm{wa}} = \mathrm{v}_{i\mathrm{wa}}\left(C_{i\mathrm{w}} - C_{i\mathrm{w}}^{\mathrm{eq}}\right) \quad \text{with} \quad C_{i\mathrm{w}}^{\mathrm{eq}} = \frac{C_{i\mathrm{a}}}{K_{i\mathrm{aw}}} \tag{19-1a}$$

where C_{iw} is the concentration of chemical i in water, and C_{iw}^{eq} is the aqueous concentration in equilibrium with the concentration in air, C_{ia}. The general equilibrium concentration ratio, R_{i21}, becomes the nondimensional Henry coefficient, K_{iaw}, also called the air–water partition constant (Eq. 9-15). Although we use the common term "air–water" exchange, in Eq. 19-1*a*, F_{iwa} is defined to be positive if the net flux is directed from water to air.

The air–water exchange velocity, v_{iwa}, refers to the situation when the flux is expressed in terms of the concentration in water. In some cases, it will be more convenient to express the flux by the concentration in air. By multiplying the concentration difference by K_{iaw} and dividing v_{iwa} by K_{iaw}, Eq. 19-1*a* turns into an analog of Eq. 18-16:

$$F_{iwa} = v_{iwa}^{*}\left(C_{ia}^{eq} - C_{ia}\right) \quad \text{with} \quad C_{ia}^{eq} = K_{iaw}C_{iw}; \quad v_{iwa}^{*} = \frac{v_{iwa}}{K_{iaw}} \tag{19-1b}$$

Smooth vs. Rough Water Surface

The remainder of this chapter focuses on the problem of determining the size of the exchange velocity, v_{iwa} or v_{iwa}^{*}, as a function of the physicochemical properties of the chemical i and the physical processes at the air–water interface. In Chapter 18, we learned that at every interface boundary a zone exists where transport is determined by the molecular diffusion coefficients of chemical i in the two phases forming the interface, D_{ia} and D_{iw}. In case of the two-layer bottleneck model, the overall exchange velocity can be written as (see Eqs. 18-10 and 18-14):

$$\frac{1}{v_{iwa}} = \frac{1}{v_{iw}} + \frac{1}{v_{ia}K_{iaw}} \quad \text{or} \quad \frac{1}{v_{iwa}^{*}} = \frac{K_{iaw}}{v_{iw}} + \frac{1}{v_{ia}} \tag{19-2}$$

where

$$v_{iw} = D_{iw}/\delta_w; \quad v_{ia} = D_{ia}/\delta_a \tag{19-3}$$

In this model, the properties of the chemical are included in the diffusivities, D_{ia} and D_{iw}, and the Henry coefficient, K_{iaw}, while the physics of the interface is hidden in the boundary layer thicknesses, δ_w and δ_a. A real world application of this model is a smooth water surface physically agitated by the wind field (Fig. 19.1*a*)

In contrast, if the water surface is described as a two-sided wall boundary, the relevant equations are (see Eq. 18-21):

$$v_{iwa} = \left(\frac{1}{\pi t^{exp}}\right)^{1/2}\left(\frac{1}{\sqrt{D_{iw}}} + \frac{1}{K_{iaw}\sqrt{D_{ia}}}\right)^{-1}$$

or (19-4*a*)

$$v_{iwa}^{*} = \left(\frac{1}{\pi t^{exp}}\right)^{1/2}\left(\frac{K_{iaw}}{\sqrt{D_{iw}}} + \frac{1}{\sqrt{D_{ia}}}\right)^{-1}$$

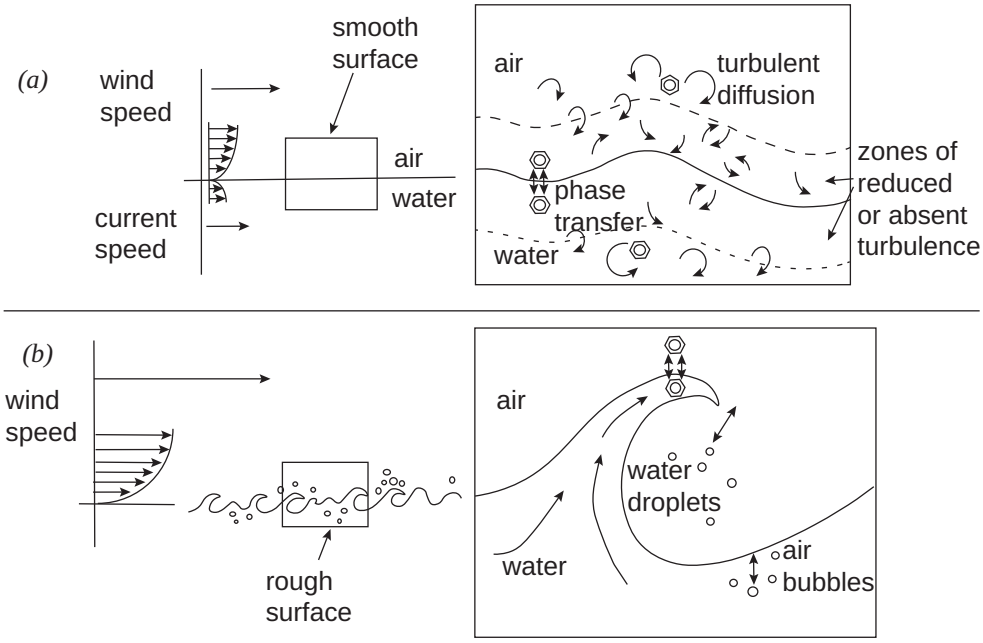

Figure 19.1 Physical conceptualizations of the air–surface water interface. (*a*) For calm conditions, the surfaces are continuous, and the horizontal velocities of the air and water on either side of the interface decrease toward the boundary. The turbulent eddies become smaller and disappear completely at the interface (boundary layer characteristics). (*b*) Larger wind speeds cause rough conditions and discontinuous water surfaces. Breaking waves cause bubbles to be pushed into the water and aerosols to be sprayed into the atmosphere. Generally, the resultant air–water interfaces do not last long enough to reach chemical equilibrium between the air and water phases.

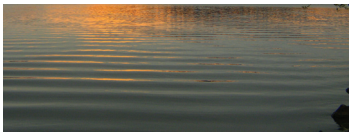

Smooth air–surface water interface. Photo: Wiberg (2007).

Rough air–surface water interface. Photo: Satoh (2008).

Here, the physics of the interface is hidden in t^{exp}, the exposure time, which is the average lifetime of a newly formed contact surface between water and air. The interface is viewed as a rough, constantly changing boundary formed by breaking waves, air bubbles, and water droplets, as shown in Fig. 19.1*b*. Since we have tacitly assumed that the exposure time is the same in air as in water, Eq. 19-4*a* has only one adjustable parameter; in contrast, Eq. 19-3 has two (δ_a and δ_w). As measurements show, reality is more complex (Section 19.3). Thus, we may need a modified version of Eq. 19-4*a* that allows for different exposure times, t_a^{exp} and t_w^{exp}:

$$v_{iwa} = \left(\frac{1}{\pi}\right)^{1/2} \left(\sqrt{\frac{t_w^{exp}}{D_{iw}}} + \frac{1}{K_{iaw}} \sqrt{\frac{t_a^{exp}}{D_{ia}}} \right)^{-1} \qquad (19\text{-}4b)$$

19.2 Air–Water Exchange Models

Air–water exchange models used to understand and describe the process have a long history with the first attempts having their roots in the design of chemical production lines (Lewis, 1916; Lewis and Whitman, 1924). These attempts recognized that chemical transfers at gas–liquid interfaces are governed by a complex combination of molecular diffusion and turbulent transport. Since no computer existed at the time, the modeling of the real physics at the interface was beyond the capability of physicists and engineers, and investigators concentrated on extrapolating an experimentally determined exchange velocity of a compound *i* in relation to the velocity of another compound *j*. This approach reduced the problem to the question: how do the compound-specific properties (molecular diffusivity and Henry's law coefficient) affect the exchange rate?

Air–Water Exchange: Compound and Fluid Specific Properties

Compounds with Air–Water Exchange Velocities Controlled by One Phase. To simplify the interpretation of exchange velocity measurements, investigations focused on two types of "reference" molecules: water in air and O_2 and CO_2 in water. Obviously, the process of evaporation or condensation of water molecules at the water surface depends on its transport through air just above the interface and not in the liquid water, thus controlling the air-side exchange velocity, v_{ia}. Box 19.1 explains how water evaporation rates and v_{ia} are related. For the water-side exchange velocity, v_{iw}, values originate from O_2 and CO_2 molecules, which have large K_{iaw} values. From these investigations, typical values of one-film exchange velocities are:

$$v_{ia}^{typical} \approx 1\ cm\ s^{-1}; \quad v_{iw}^{typical} \approx 10^{-3}\ cm\ s^{-1} \tag{19-5}$$

With these values, we can determine the critical nondimensional Henry's law coefficient, $K_{iaw}^{critical}$, for which the contributions from the two boundary layers, air and water, are approximately equal. From Eq. 19-2:

$$K_{iaw}^{critical} \approx \frac{v_w^{typical}}{v_a^{typical}} = 10^{-3} \tag{19-6}$$

Box 19.1 Estimating Air Phase Exchange Velocity from Evaporation of Water

Traditionally, water is used as the test substance for determining the air phase exchange velocity, v_{ia}. At 25°C, the concentration of water vapor in air at saturation (100% relative humidity) is $C_{H_2O\,a}^{eq} = 23.0\ g_{H_2O}\ m_a^{-3}$ (Appendix B.3, Table B.3*a*). Since 1 m^3 of water contains 10^6 g of water, the air–water equilibrium ratio at 25°C is $K_{H_2O\,aw} = 2.3 \times 10^{-5}$. This value is much smaller than $K_{aw}^{critical}$ (Eq. 19-6), thus one can reasonably expect that evaporation of water is air-side controlled. We use Eq. 19-1*b* and reverse the sign such that $F_{evap} > 0$ means *evaporation* (then $F_{evap} < 0$ means *condensation* of water vapor at the water surface):

$$F_{evap} = v_{H_2O\,wa}^{*}\left(C_{H_2O\,a}^{eq} - C_{H_2O\,a}\right) = v_{H_2O\,wa}^{*}\,C_{H_2O\,a}^{eq}\,(1 - RH) \tag{1}$$

where RH is the relative humidity defined as: $RH = C_{H_2O\,a}/C_{H_2O\,a}^{eq}$. Thus, the air phase velocity, $v_{H_2O\,a}$, can be determined from evaporation rates and relative humidity:

$$v_{H_2O\,a} \approx v_{H_2O\,wa}^{*} = \frac{F_{evap}}{C_{H_2O\,a}^{eq}(1 - RH)} \tag{2}$$

A typical value is $v_{ia}^{typical} \approx 1\ cm\ s^{-1}$(Eq. 19-5).

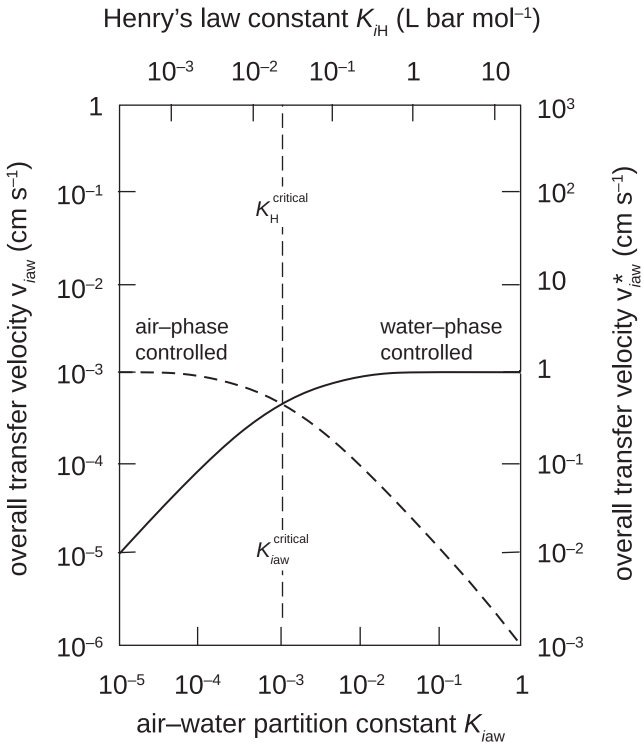

Figure 19.2 Schematic view of the overall air–water exchange velocity, v_{iwa}, as a function of the nondimensional Henry's law coefficient, K_{iaw}, calculated from Eq. 19-2 with typical single phase transfer velocities $v_{ia} = 1$ cm s^{-1} and $v_{iw} = 10^{-3}$ cm s^{-1}. The broken line shows the exchange velocity, v^*_{iwa} (Eq. 19-1*b*, air chosen as the reference system). The upper scale gives the Henry's Law coefficient at 25°C, $K_{iH} = 24.7$ (L bar mol^{-1}) $\times K_{iaw}$.

At 20°C (T = 293 K), the critical Henry's law coefficient, K_{iH}^{critical}, is about 0.025 L bar mol^{-1} (see Eq. 9-15). Thus, the substances controlled by just one phase, must have the following property:

$$\begin{aligned} &K_{iaw} \ll K_{iaw}^{\text{critical}} = 10^{-3} \quad v_{iwa} \approx K_{iaw} v_{ia} \text{ or } v^*_{iwa} \approx v_{ia} \quad \text{air phase-controlled} \\ &K_{iaw} \gg K_{iaw}^{\text{critical}} = 10^{-3} \quad v_{iwa} \approx v_{iw} \quad \text{water phase-controlled} \end{aligned} \tag{19-7}$$

In Fig. 19.2, the overall air–water exchange velocity for typical single phase velocites (Eq. 19-5) is shown as a function of the Henry's law coefficient.

Film Model. The first actual air–water exchange model, the *film model* by Whitman (1923), depicted the interface as a single- or two-layer bottleneck boundary (see Eqs. 19-2 and 19-3). Although many aspects of this model are outdated in light of our improved knowledge of the physical processes occurring at the interface, its mathematical simplicity keeps the model popular. The model predicts that for substances i and j with air–water exchange velocities that are controlled by just one boundary layer (either water-side or air-side, see Eq. 19-7), the exchange velocities and the molecular diffusion coefficients are linearly related:

$$\frac{v_{i\alpha}}{v_{j\alpha}} = \frac{D_{i\alpha}}{D_{j\alpha}} \quad \text{where } \alpha \text{ stands for air (a) or water (w)} \tag{19-8}$$

Because the diffusivity ratio, $D_{i\alpha}/D_{j\alpha}$, is not identical for air and water, and since Eq. 19-2 also contains K_{iaw}, Eq. 19-8 does not hold for chemicals with Henry coefficients close to $K_{iaw}^{\text{critical}}$.

Diffusion coefficients[a]

T (°C)	$D_{H_2O\,a}$ ($cm^2\ s^{-1}$)	D_{CO_2w} ($cm^2\ s^{-1}$)	D_{O_2w} ($cm^2\ s^{-1}$)
0	0.22	9.4×10^{-6}	9.7×10^{-6}
5	0.23	1.1×10^{-5}	1.1×10^{-5}
10	0.23	1.3×10^{-5}	1.3×10^{-5}
15	0.24	1.5×10^{-5}	1.5×10^{-5}
20	0.25	1.7×10^{-5}	1.8×10^{-5}
25	0.26	1.9×10^{-5}	2.0×10^{-5}
30	0.26	2.2×10^{-5}	2.3×10^{-5}

[a]Data from Han and Bartels (1996); Massman (1998); Yaws (2009).

Using the approximate diffusion coefficient of water vapor in air, $D_{H_2O\,a} \sim 0.3\ cm^2\ s^{-1}$, and for CO_2 in water, $D_{CO_2w} \sim 2 \times 10^{-5}\ cm^2\ s^{-1}$ (see Massman, 1998 and Yaws, 2009), as well as the approximate size of the exchange velocities given in Eq. 19-5, the implied film thicknesses are typically:

$$\delta_a = \frac{D_{H_2O\,a}}{v_{H_2O\,a}} \sim 0.3\ cm; \qquad \delta_w = \frac{D_{CO_2w}}{v_{CO_2w}} \sim 0.02\ cm \tag{19-9}$$

Surface Renewal Model. An alternative approach is the *surface renewal model* by Higbie (1935) and Danckwerts (1951). It applies to highly turbulent conditions in which new surfaces are continuously formed. Here, the interface is described as a two-sided wall boundary. The exposure times, t_a^{exp} and t_w^{exp}, determine how frequently the interfaces are replaced. The overall exchange velocity, v_{iwa}, is given by Eq. 18-4*b*. In analogy to Eq. 19-7, the total air–water exchange velocity of substances controlled by just one phase must have the following property:

$$K_{iaw} \ll K_{iaw}^{critical} \quad v_{iwa} \approx K_{iaw} v_{ia} \text{ or } v_{iwa}^* \approx v_{ia} = \left(\frac{D_{ia}}{\pi\, t_{exp}^a}\right)^{1/2} \quad \text{air phase-controlled}$$

$$K_{iaw} \gg K_{iaw}^{critical} \quad v_{iwa} \approx v_{iw} = \left(\frac{D_{iw}}{\pi\, t_{exp}^w}\right)^{1/2} \quad \text{water phase-controlled} \tag{19-10}$$

Using the same reference compounds (water vapor and CO_2) and the same typical exchange velocities as in the film model (Eq. 19-5), the exposure times for the air and water phase are approximately:

$$t_{exp}^a = \frac{D_{H_2O\,a}}{\pi\, v_{H_2O\,a}^2} \sim \frac{0.3\ cm^2\ s^{-1}}{3\ (1\ cm\ s^{-1})^2} = 0.1\ s; \quad t_{exp}^w = \frac{D_{CO_2w}}{\pi\, v_{CO_2w}^2} \sim \frac{2 \times 10^{-5}\ cm^2\ s^{-1}}{3 \cdot (10^{-3}\ cm\ s^{-1})^2} \sim 7\ s \tag{19-11}$$

These results suggest that the air is replaced more often than the water. Given the different densities and viscosities of the air and water, this is not an unreasonable result.

The surface renewal model predicts that for substances *i* and *j* with air–water exchange velocities that are controlled by just one boundary layer (either water-side or air-side, see Eq. 19-10), the exchange velocities and the molecular diffusion coefficients are related by:

$$\frac{v_{i\alpha}}{v_{j\alpha}} = \left(\frac{D_{i\alpha}}{D_{j\alpha}}\right)^{1/2} \qquad \text{where } \alpha \text{ stands for air or water} \tag{19-12}$$

with an exponent of 1/2 in contrast to 1 in the film model (Eq. 19-8).

Boundary Layer Model. In the 1970s, the growing interest in global geochemical cycles and the fate of man-made pollutants in the environment triggered numerous

studies of air–water exchange in natural systems, especially between the ocean and the atmosphere. In micrometeorology, the study of heat and momentum transfer at water surfaces led to the development of detailed models of the structure of turbulence and momentum transfer close to the interface. The best-known outcome of these efforts, Deacon's (1977) *boundary layer model*, is similar to Whitman's film model. However, Deacon replaced the step-like drop in diffusivity (see Fig. 18.2) by a continuous profile where diffusivity gradually decreases from the interior of the compartment to the boundary. Deacon concluded that mass transfer at the interface must be controlled by the simultaneous influence of two related processes, that is, by the transport of chemicals described by molecular diffusivity, $D_{i\alpha}$(the subscript α stands for the fluid medium, air or water), and by the transport of turbulence described by the coefficient of kinematic viscosity, ν_α, having the same dimensions as $D_{i\alpha}$. The ratio between these two quantities is nondimensional and is called the *Schmidt Number*, $\mathrm{Sc}_{i\alpha}$:

$$\mathrm{Sc}_{i\alpha} = \frac{\nu_\alpha}{D_{i\alpha}} \quad \text{where } \alpha \text{ stands for air or water} \tag{19-13}$$

Deacon derived his model for compounds with large Henry's law coefficients for which the air–water transfer velocity solely depends on the conditions in the water phase. The model leads to an expression of the form:

$$\mathrm{v}_{i\mathrm{w}} = \text{constant}\,(\mathrm{Sc}_{i\mathrm{w}})^{-n} = \text{constant}\,\nu_{\mathrm{w}}^{-n} D_{i\mathrm{w}}^{n} \tag{19-14}$$

In Deacon's original theory, the exponent n was equal to 2/3. According to Eq. 19-14, $\mathrm{v}_{i\mathrm{w}}$ increases for decreasing ν_w and for increasing $D_{i\mathrm{w}}$ where the exponent of the latter lies between the exponent of the surface renewal model ($n = 1/2$) and the film model ($n = 1$). The exchange velocity would remain unchanged if both viscosity and diffusivity increase or decrease by the same relative amount. More recently, Mackay and Yeun (1983) also developed expressions for $\mathrm{v}_{i\mathrm{a}}$ that depend on $\mathrm{Sc}_{i\mathrm{a}}$ raised to the 2/3 power.

The following situation may help us to understand this result, at least qualitatively. Imagine a border between two states which, for whatever reason, can only be crossed on foot. People use taxis to get to the border; yet when approaching the border, the streets become increasingly narrow, and the cars get stuck. The passengers in the taxis know exactly the optimal time to jump out of the cars in order to walk or run the remaining distance and to cross the border after the shortest possible time. Obviously, the distance from the border where people leave the taxis is not the same for all persons and all road conditions. People who are fast runners (that is, have "large diffusivities") leave the cars earlier than people who walk with difficulty ("small diffusivities"). However, a person's speed is not the only determinant for the optimal jumping point; in some areas, the roads leading to the border are narrower and thus more strongly congested ("large viscosity" damping the motion of the cars, that is, the turbulent eddies); in other areas, the roads are broader (small viscosity).

This picture makes the air–water exchange dependency on the Schmidt Numbers, $\mathrm{Sc}_{i\mathrm{w}}$ and $\mathrm{Sc}_{i\mathrm{a}}$, plausible, although it obviously does not explain the size of the exponent in Eq. 19-14. In Deacons' theory, strictly speaking, this exponent is only valid for a rigid

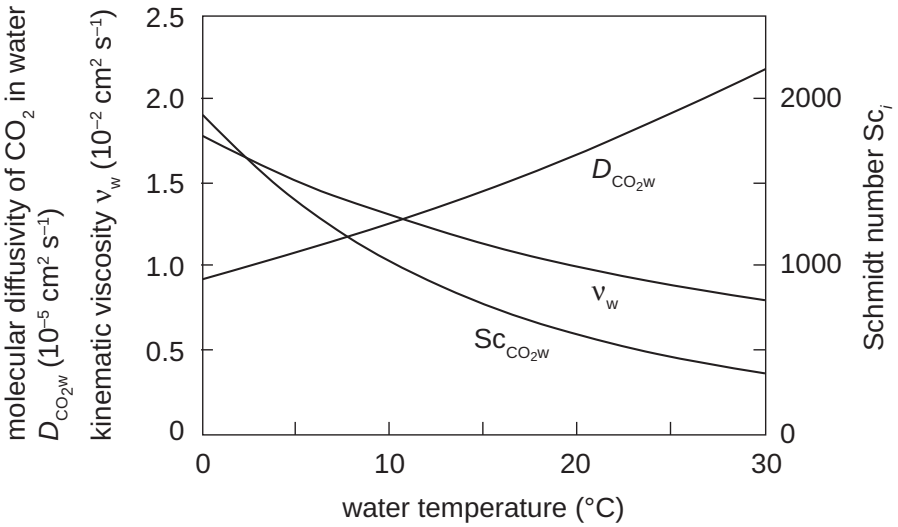

Figure 19.3 Variation with water temperature of kinematic viscosity, ν_w, aqueous diffusivity of CO_2, D_{CO_2w}, and Schmidt number, $Sc_{CO_2w} = \nu_w / D_{CO_2w}$.

wall (a motionless water surface). As shown by Jähne et al. (1987b), the exponent changes to $n = 1/2$ at larger wind speeds. The transition takes place at wind speeds of about 5 m s^{-1} (Liss and Merlivat, 1986). However, the effect of wind speed on v_{iw} and v_{ia} is *indirect*; the main influence is hidden in the constant of Eq. 19-14. Before we have a closer look at the physical forces, like wind, that influence the size of v_{iwa}, let us briefly discuss the influence of temperature and salinity.

Sc of CO_2 in fresh water and in seawater[a]

T (°C)	Sc_{CO_2w}	$Sc_{CO_2seawater}$
0	1910	2070
10	1030	1140
20	600	670
30	360	400

[a]Data from Wanninkhof (1992).

Boundary Layer Model: Influence of Fluid Temperature and Salinity on v_{iw}. Since diffusivities increases and fluid viscosities decrease with temperature, Schmidt numbers also decrease with temperature. For example, between 0 and 30°C, Sc_{iw} values decrease by more than a factor of 3 (Fig. 19.3 and Table 19.1). Since the kinematic viscosity of seawater is greater than that of freshwater, Schmidt numbers are about 10% higher in seawater than in fresh water (see table). Wanninkhof (1992) provides empirical expressions for estimating Schmidt numbers for 13 volatile chemicals including CO_2 and O_2 in both freshwater and seawater at temperatures between 0 and 30°C.

Depending on the exponent n that relates v_{iw} to Sc_{iw} (Eq. 19-14), the effect on v_{iw} of temperature and salinity variations between 0 and 30°C, and from 0 to 35 psu amounts to a factor of 5 to 10. This effect is greatly underestimated in the classical film and surface renewal models that omit the influence of viscosity. In turn, the variation of Sc_{iw} between different chemicals, for example, helium and benzene, *at a fixed temperature and salinity* can also amount to a factor of 10. This influence is solely due to the differences in the molecular diffusivities of these substances, and hence an effect that is also taken into account by the other models. In short, the film and surface renewal models are adequate to deduce the air–water exchange velocity of a substance from the velocity of another substance *measured at the same temperature and salinity*. However, they are not capable to take into account the effect of temperature and salinity on the exchange velocity of a substance.

Table 19.1 Kinematic Viscosities[a], Molecular Diffusivities[b], and Schmidt Numbers (Sc_{iw}) in Water for Selected Chemicals

	Viscosity	Oxygen (O_2)		Carbon Dioxide (CO_2)		Methane (CH_4)		Helium (He)		Benzene	
T (°C)	ν_w ($cm^2\ s^{-1}$)	D_{iw} ($cm^2\ s^{-1}$)	Sc_{iw} (–)	D_{iw} ($cm^2\ s^{-1}$)	Sc_{iw} (–)	D_{iw} ($cm^2\ s^{-1}$)	Sc_{iw} (–)	D_{iw} ($cm^2\ s^{-1}$)	Sc_{iw} (–)	D_{iw} ($cm^2\ s^{-1}$)	Sc_{iw} (–)
0	1.79×10^{-2}	1.11×10^{-5}	1600	0.93×10^{-5}	1910	0.94×10^{-5}	1890	4.74×10^{-5}	380	0.39×10^{-5}	4600
5	1.52	1.3	1170	1.09	1390	1.09	1390	5.20	290		
10	1.31	1.52	860	1.26	1040	1.25	1050	5.68	230		
15	1.14	1.77	640	1.46	780	1.43	800	6.19	180		
20	1.00	2.05	490	1.68	600	1.63	610	6.73	150		
25	0.89	2.36	380	1.92	470	1.85	480	7.30	120	1.06×10^{-5}	840
30	0.80	2.70	300	2.18	370	2.09	380	7.89	100		

[a]Data from Appendix B.3, Table B.3*a* and B.3*b*.
[b]Data from Himmelblau (1964); Jähne et al. (1987a); and Oelkers (1991).

Air–Water Exchange: The Physics of the Water Surface

In the previous discussion, we identified the properties of chemicals and fluids (air and water) that influence the size of air–water exchange. Now, we turn our attention to the external driving forces. Intuitively, we expect that agitating the water surface enhances air–water exchange. Obviously, in standing waterbodies (ocean and lakes), the most important driving force for stirring is the wind. In rivers, the flow velocity is an additional source of turbulence, perhaps the dominant one. Therefore, investigators who have studied air–water exchange in standing surface waters have always tried to find simple relationships between either wind speed and v_{iwa} or flow velocity and v_{iwa}.

As is shown, under certain conditions such simple approaches often work quite well, although neither the wind nor the flow velocity of the water influences directly the processes at the water surface and thus the size of v_{iwa}. In fact, the physical processes at the water surface are determined by the level of turbulent kinetic energy in the water column. In fluid dynamics, turbulent kinetic energy is usually expressed by a parameter with the dimension of a velocity, u^*. Three main sources of turbulent kinetic energy exists in a waterbody, (1) turbulence introduced by the wind (quantified by the wind-induced friction velocity, u^*_W), (2) turbulence introduced by convective motion due to density instabilities in the water column resulting, for instance, from cooling of the water (convective turbulent velocity, u^*_C), (3) turbulence introduced by the friction of the flowing water at the sediment surface in rivers and estuaries exposed to tidal motion (shear velocity, u^*_F, the subscript F stands for flow).

Chu and Jirka (2003), based on laboratory experiments that involved both stream flow and wind, analyzed the relative importance of the turbulent velocities on v_{iw} for different current and wind speeds. They proposed an *additive* model:

$$v_{iwa} = v_{iwa}(u^*_W) + v_{iwa}(u^*_F) + v_{iwa}(u^*_C) \tag{19-15}$$

where the parentheses on the right-hand side of the expression point to the origin of turbulence that contributes to the air–water exchange velocity. For instance, in

oceans and deep lakes exposed to strong winds, only the first term is important, in fast flowing rivers only the second one. The third contribution can become important in lakes with little wind exposure where air–water exchange velocities in fall when the water column is cooling is usually greater than in spring when lake stratification suppresses convective motion.

In the remaining sections we look at "pure" cases, that is, at situations where either wind-induced turbulence (Section 19.3) or flow-induced turbulence (Section 19-4) is the only relevant source of turbulence. Even if one source of turbulence is dominant, the relation between the size of the source (e.g., wind speed) and v_{iwa} is not necessarily the same for all waterbodies since waves and currents produced by the wind strongly depend on the size and depth of the waterbody and on other factors, e.g., wind direction (wind across versus wind along the waterbody).

19.3 Measurement of Air–Water Exchange Velocities

Exchange Velocities in Air

As mentioned earlier, the exchange velocity for water vapor, $v_{H_2O\,a}$, is used as the reference molecule of the air-side exchange velocity, v_{ia} (Box 19.1). This value is then transformed for other chemicals with the help of one of the discussed models (Eqs. 19-8 and 19-12). Hydrologists have long recognized the relationship between $v_{H_2O\,a}$ and environmental factors such as wind speed, u (Dalton, 1802; Rohwer, 1931; Sverdrup et al., 1942). In laboratory experiments, many investigators showed that increasing wind speed enhances $v_{H_2O\,a}$ approximately linearly (Penman, 1948; Liss, 1973; Münnich et al., 1978; Mackay and Yeun, 1983). All these relationships resulted in linear models of the form:

$$v_{H_2O\,a}(\mathrm{cm\,s^{-1}}) = A + B\,u_{10}(\mathrm{m\,s^{-1}}) \tag{19-16}$$

where u_{10} is wind speed measured 10 m above the water surface or extrapolated to this height. It is now believed that such lab results typically overestimate the magnitude of the parameters A and B (Mackay and Yeun, 1983). Many investigators assumed A to be zero. For instance, Fairall et al. (1996, 2003, 2011) observed $B \sim 0.11$ for winds between 2 and 18 m s^{-1}, but Mackay and Yeun (1983) noted that $v_{H_2O\,a}$ still has a value near 1 cm s^{-1}, even in cases with no wind ($A = 1$ cm s^{-1}). Oost et al. (2000) found that in cases where the temperature of the lower atmosphere was greater than the temperature of air adjacent to the surface water (i.e., stable stratification across the air–water interface), the parameter B may decrease to only about 0.03. This implies that if the water temperature is greater than the air temperature, significant heat transfers from water to the air may be involved, causing buoyancy in air that enhances vertical transport, even in the absence of wind. As a result, Johnson (2010) proposed a baseline value should be added to the wind dependency function:

$$v_{H_2O\,a}(\mathrm{cm\,s^{-1}}) = 0.1 + 0.11\,u_{10}(\mathrm{m\,s^{-1}}) \tag{19-17}$$

Fairall et al. (1996, 2003) and Johnson (2010) developed a more complex formulation that includes the effect of changing the air's drag coefficient with wind speed and phenomena like wind gustiness. This "physics based" approach is based on the theory of wind friction in a boundary layer and is called the Coupled Ocean-Atmosphere Response Experiment (COARE) model. With only a limited number of coefficients tuned to fit field observations (Jeffery et al., 2010), this model has the following complex dependencies on wind speed (after Johnson 2010):

$$v_{H_2O\,a}(\mathrm{cm\,s^{-1}}) = 0.1 + \frac{u_{10}(6.1 + 0.63u_{10})^{0.5}}{13.3\,(Sc_{H_2O\,a})^{0.5} + (6.1 \times 10^{-4} + 6.3 \times 10^{-5}u_{10})^{-0.5} - 5 + 1.25\,\ln Sc_{H_2O\,a}} \quad (19\text{-}18)$$

where $Sc_{H_2O\,a}$ is the Schmidt Number of water vapor in air (Eq. 19-13).

Using Eq. 19-18 and the Schmidt number for water in air at 20°C, $Sc_{H_2O\,a}$= 0.6, we can estimate $v_{H_2O\,a}$ as a function of wind speed, which increases smoothly from 0.1 cm s^{-1} at no wind up to almost 3 cm s^{-1} at u_{10} of 20 m s^{-1}. Until about 10 m s^{-1}, the simple formulation deduced from field studies of water evaporation (Eq. 19-17) compares favorably to the physics-based COARE model (see Fig. 19.4).

Using such simple models of $v_{H_2O\,a}$, we can now estimate fluxes of organic compounds like methanol that have Henry constants that are well below the critical value (recall

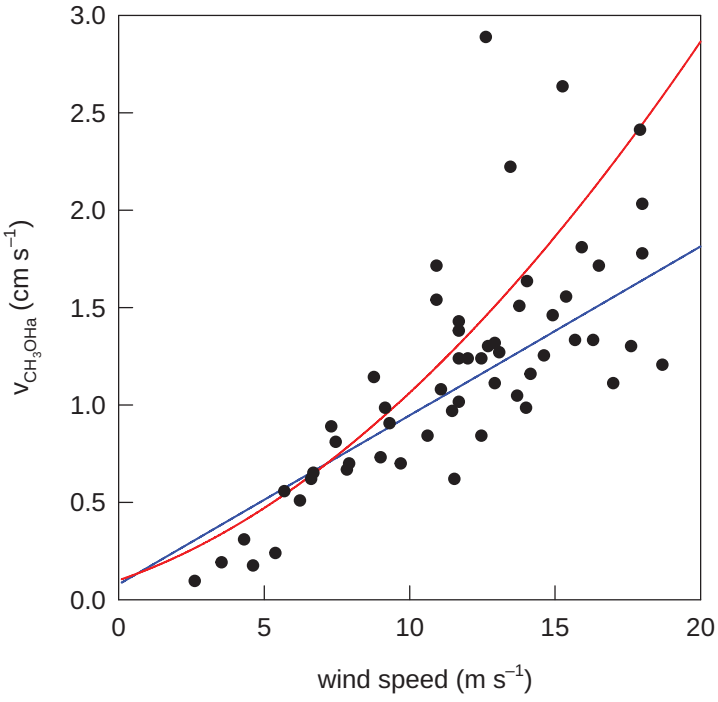

Figure 19.4 Comparison of measured methanol (K_{iaw} = 2 × 10^{-4}) transfer velocities, v_{CH_3OHa}, versus wind speeds at 10 m (6 h running average) for surface ocean–atmosphere exchanges (Yang et al., 2014) with estimates based on the COARE model (red line; Eq. 19-18; Fairall et al., 2003) and the linear model (blue line, Eq. 19-17).

Box 19.2 Estimating Air Phase Exchange Velocity from Evaporation Rates of Pure Organic Liquids

Mackay and van Wesenbeeck (2014) correlated evaporation rates from pure organic liquids, $F_{i\text{evap}}$, with vapor pressure, $p^*_{i\,\text{L}}$, for about 50 organic compounds with molar mass M_i between 30 and 400 g mol^{-1} and vapor pressure between 4×10^{-5} and 3×10^4 Pa finding the linear correlation ($T = 25°\text{C}$):

$$F_{i\text{evap}}(\text{mol m}^{-2}\text{s}^{-1}) = \text{constant}\, p^*_{i\text{L}}\,(\text{Pa}) \text{ with constant} = 3.17 \times 10^{-7} \text{mol m}^{-2}\text{s}^{-1}\,\text{Pa}^{-1} \tag{1}$$

The concentration of chemical i in the air at the interface above the liquid, $C^{\text{eq}}_{i\text{a}}$, is related to its saturation vapor pressure, $p^*_{i\,\text{L}}$, by:

$$C^{\text{eq}}_{i\text{a}} = \frac{p^*_{i\text{L}}}{RT} \tag{2}$$

The equations in Box 19.1 derived for the evaporation of water can also be applied here. By assuming that the vapor pressure of the chemical at some distance from the liquid is zero, we get:

$$F_{i\text{evap}} = \text{v}_{i\text{a}} C^{\text{eq}}_{i\text{a}} = \text{v}_{i\text{a}} \frac{p^*_{i\text{L}}}{RT} \tag{3}$$

By combining Eqs. 1 and 3, we get the average air phase exchange velocity of the chemicals, $\bar{\text{v}}_{i\text{a}} = 3.17 \times 10^{-7}\,\text{mol m}^{-2}\text{s}^{-1}\text{Pa}^{-1} \times RT = 0.078\,\text{cm s}^{-1}$

If we want to compare this value with the exchange velocity found for water vapor (e.g., Eq. 19-17), we have to take into account that $\text{v}_{i\text{a}}$ of an individual compound i also depends on its diffusion coefficient in air, $D_{i\text{a}}$, and recognize that the viscosity of the air drops out from Eq. 19-19:

$$\text{v}_{i\text{a}} = \left(\frac{\text{Sc}_{i\text{a}}}{\text{Sc}_{\text{H}_2\text{Oa}}}\right)^{-2/3} \text{v}_{\text{H}_2\text{O a}} = \left(\frac{D_{i\text{a}}}{D_{\text{H}_2\text{Oa}}}\right)^{2/3} \text{v}_{\text{H}_2\text{O a}} \tag{4}$$

Recalling that the diffusivity of water vapor in air is 0.26 cm^2 s^{-1} and for small organic compounds, $D_{i\text{a}} \approx 0.1$ cm^2 s^{-1}, we estimate:

$$\text{v}_{\text{H}_2\text{O a}} = 0.078\,\text{cm s}^{-1} \left(\frac{D_{i\,\text{H}_2\text{Oa}}}{D_{i\text{a}}}\right)^{2/3} = 0.078\,\text{cm s}^{-1} \left(\frac{0.26}{0.1}\right)^{2/3} = 0.15\,\text{cm s}^{-1} \tag{5}$$

This result is somewhat larger than found using the relationship in Eq. 19-17 for $u_{10} = 0$, again emphasizing the tendency for laboratory data to yield $\text{v}_{\text{H}_2\text{O a}}$ values that are somewhat higher than those measured in the field.

Eq. 19-6). The air-side exchange velocity of a compound *i* like methanol can then be estimated from (see Eq. 19-14):

$$v_{ia} = \left(\frac{Sc_{ia}}{Sc_{H_2Oa}} \right)^{-2/3} v_{H_2Oa} \qquad (19\text{-}19)$$

where the exponent $n = -2/3$, as suggested by Mackay and Yeun (1983) and Johnson (2010). Given the precision with which field measures of fluxes of compounds like methanol can be measured (Yang et al., 2014), both the complex COARE model and the simpler linear model give reasonable results (Fig. 19.4).

In Box 19.2, another prominent example of a gas phase-controlled exchange flux is discussed: the measurement of evaporation rates from pure organic liquids. Applying the method to laboratory data by Mackay and van Wesenbeeck (2014) yields $v_{ia} \approx 0.08$ cm s^{-1}, about 80% of the "zero-wind" value of Eqs. 19-17 and 19-18. In fact, when correcting for the influence of molecular diffusivity in air on v_{ia}, evaporation data from pure organic liquids yield results that agree well with the data from evaporation of water.

Water Phase Exchange Velocities Deduced from Compounds with Large Henry's Law Constants

As a next step, we analyze experimental information on air–water exchange for substances for which only the water phase exchange velocity is relevant. According to Eq. 19-7, we find the substances have Henry's law constant $K_{iaw} \gg K_{iaw}^{critical} = 10^{-3}$ like O_2, CO_2 and all noble gases. Early workers on air–water exchange pursued laboratory experiments for O_2 or CO_2 (e.g., Kanwisher, 1963; Liss, 1973) while later geochemical investigations included natural radioactive tracers such as ^3He and ^{222}Rn (Broecker and Peng, 1971; Emerson et al., 1973; Peng et al., 1979; Torgersen et al., 1982; Jähne et al., 1987b) and artificial chemical tracers such as SF_6 (Wanninkhof et al., 1987). With the growing debate on climate change, the development of global CO_2 models moved into the focus of oceanography, and investigations on air–water exchange became more focused on the exchange of CO_2 at the surface of the ocean.

Influence of Wind Speed on Air–Water Exchange. In Section 19.2, we discussed the influence of turbulence in the water on the water-phase exchange velocity, v_{iw}. We have noted that wind forcing is one, but not the only, source of turbulence (Eq. 19-15). The existence of other sources of turbulence, like water currents and convective motion, makes it difficult, if not impossible, to develop one simple, generally valid model allowing accurate predictions of v_{iw} for oceans, estuaries, lakes, or rivers based on just a few parameters such as average wind speed or flow velocity. The situation is less complex if one of the several turbulence producing mechanisms dominates. In rivers, this usually is the stream current (see Section 19.4). In oceans, estuaries, and lakes, it may be the wind, provided that the wind speed, u_{10}, exceeds a threshold of 5 to 10 m s^{-1}.

Many investigators have made field measurements of exchange velocities of CO_2 between surface waters and the atmosphere. McGillis et al. (2001) proposed an equation that includes a constant value for small wind velocities plus a third-power function in u_{10}:

$$v_{iw}(\text{cm s}^{-1}) = \left(9\times10^{-4} + 7.2\times10^{-6}\ \left[u_{10}(\text{m s}^{-1})\right]^3\right)\left(\frac{Sc_{iw}}{660}\right)^{-1/2} \qquad (19\text{-}20)$$

where v_{ia} is the exchange velocity and Sc_{iw} the Schmidt number (Eq. 19-13) for the chemical i in water. The exponent for the Schmidt number ratio ($n = 1/2$) indicates that the model is based on the modified boundary layer theory by Deacon (1977) as discussed by Ledwell (1984). The reference Schmidt number ($Sc_{iw} = 660$) corresponds to CO_2 in *seawater* at 20°C.

Moslashrk et al. (2014) and Vachon and Prairie (2013) found similar relations for estuaries and lakes. The constant factor (v_{iw} for $u_{10} = 0$) is larger than for the ocean, but the fits are far worse than for oceans. This shows, as previously mentioned, that additional factors are affecting the influence of winds in these smaller surface water systems. For estuaries, there is a significant influence of the water's current on the air–water interface. For lakes, the situation is particularly complicated by factors such as wind fetch and surface water convection. Read et al. (2012) found that convective mixing of the surface layers in lakes becomes increasingly important as lakes become smaller than about 1 km^2. As a result, the water boundary layer behaviors can be different, and air–water exchanges greater than expected by only considering the wind speed.

In Fig. 19.5, adapted from Johnson (2010), the expression by McGillis et al. (2001) (Eq. 19-20) is compared to various other models and to measurements for wind speeds between 0 and 7 m s^{-1}. The important lesson from these data is that, particularly at small wind speed, prediction of air–water exchange from wind speed alone should be handled with great care since the values may be wrong by up to a factor of ten. This may be sufficient to assess the order of magnitudes of different processes that affect a particular chemical, but for more refined predictions, field observations for the particular waterbody may be necessary.

Influence of Waves at High Wind Speeds. The influence of the waves becomes particularly evident at wind speeds above about 10 m s^{-1}, that is, above the onset of wave breaking and formation of air bubbles (Blanchard and Woodcock, 1957; Monahan, 1971; Kolovayev, 1975; Johnson and Cooke, 1979; Wu, 1981). In this range, transfer velocities determined from natural systems may be distorted by an additional effect called *wind pumping*. In this situation, bubbles are injected deep below the water surface and experience pressures in excess of atmospheric. As a result, larger quantities of the chemicals contained in the bubbles are dissolved in the water than are required for equilibrium at the water surface. This leads to supersaturation of O_2, N_2, and CO_2 of up to 15% (Smith and Jones, 1985; Stanley et al., 2009). This process not only influences the size of v_{iw}, but it may also invalidate the general form of Eq. 19-1 according to which the sign of the net air–water flux is determined by the

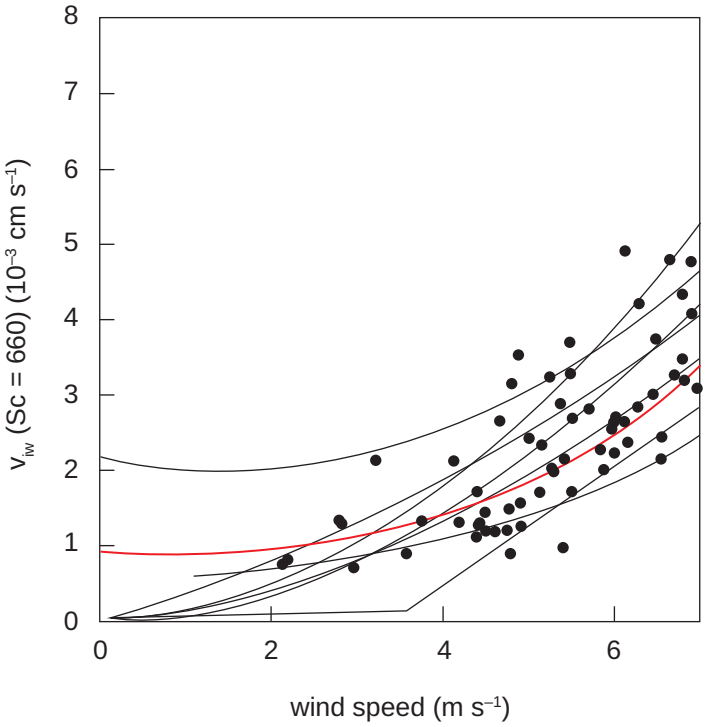

Figure 19.5 Comparison of different measurements and models (lines) of the water-side air–water exchange velocity, v_{iw}, for small wind speed as a function of wind speed u_{10} (m s^{-1}) valid for Schmidt number $Sc_{iw} = 660$ (CO_2 in seawater at 20°C), adapted from Johnson (2010). The expression proposed by McGillis et al. (2001) (Eq. 19-20) is shown by the red line.

sign of the concentration difference ($C_{iw} - C_{iw}^{eq}$). In order to produce supersaturation, F_{iaw} must be directed into the water ($F_{iaw} < 0$), even if C_{iw} is larger than C_{iw}^{eq}.

Overall Air–Water Exchange Velocities

The foregoing discussion has demonstrated that the physics of air–water exchange is extremely complex and likely strongly dependent on the environmental setting. The combination of different system-specific and substance-specific influences on v_{iwa} and the mismatch of time scales of the external forcing (wind) and of the system's response may explain why observations in the laboratory and field have never correlated with the unique model, which early investigators hoped to achieve. Although it is important to realize that experimental data often are ambiguous, we should not be discouraged from developing useful recipes for estimating overall air–water transfer velocities for different environmental conditions and different compounds. In Box 19.3, a summary of such recipes is attempted that can be used whenever more refined data on the physics of the air–water interface are missing.

Box 19.3 Summary of Simple Recipes to Calculate Overall Air–Water Exchange Fluxes

$$F_{iwa} = v_{iwa}(C_{iw} - C_{iw}^{eq}) \quad \text{with} \quad C_{iw}^{eq} = \frac{C_{ia}}{K_{iaw}} \tag{19-1a}$$

$$\frac{1}{v_{iwa}} = \frac{1}{v_{iw}} + \frac{1}{v_{ia}K_{iaw}} \tag{19-2}$$

where u_{10} is in (m s^{-1}), v_{iwa}, v_{ia} and v_{iw} are in (cm s^{-1}), and F_{iwa} is the flux, positive if directed from water to air; K_{iaw} is the nondimensional Henry's law coefficient.

Air phase velocity

Reference molecule: water vapor at 25°C

Simple:

$$v_{H_2O\,a}(\text{cm s}^{-1}) = 0.1 \; + \; 0.11\; u_{10}(\text{m s}^{-1}) \tag{19-17}$$

More complex (COARE model):

$$v_{H_2O\,a}(\text{cm s}^{-1}) = 0.1 + \frac{u_{10}(6.1 + 0.63u_{10})^{0.5}}{13.3\;(Sc_{H_2O\,a})^{0.5} + (6.1 \times 10^{-4} + 6.3 \times 10^{-5}u_{10})^{-0.5} - 5 + 1.25\;\ln\,Sc_{H_2O\,a}} \tag{19-18}$$

where $Sc_{H_2O\,a}$ is the Schmidt Number of water vapor in air (Eq. 19-13) and u_{10} is wind speed 10 m above water surface in m s^{-1}.

For compound i:

$$v_{ia} = \left(\frac{Sc_{i\,a}}{Sc_{H_2Oa}}\right)^{-2/3} v_{H_2O\,a} \tag{19-19}$$

Water phase velocity

Reference molecule: CO_2 in seawater at 20°C ($Sc_{iw} = 660$):

$$v_{iw}(\text{cm s}^{-1}) = \left(9 \; \times \; 10^{-4} + 7.2 \; \times \; 10^{-6} \; \left[u_{10}(\text{m s}^{-1})\right]^3\right)\left(\frac{Sc_{iw}}{660}\right)^{-1/2} \tag{19-20}$$

Linear Air–Water Exchange Rate Constants

With the one-box model developed in Section 6.2, we can describe the effect of the air–water exchange flux on the concentration of chemical i in a system with volume V. The procedure is described in Box 19.4. The resulting equation is the same as the one derived for describing the effect of particle sedimentation (Eqs. 12-26 to 12-28).

Box 19.4 Calculation of Linear Air–Water Exchange Rate Constants

We consider an aqueous system with volume V and air–water interface area A_o. Then the effect on total mass of chemical i in the system, $\mathcal{M}_{iw}$, is (Eq. 6-2):

$$\frac{d\mathcal{M}_{iw}}{dt} = -A_o F_{iwa} = -A_o v_{iwa}(C_{iw}^{surface} - C_{iw}^{eq}) \quad \text{with} \quad C_{iw}^{eq} = \frac{C_{ia}}{K_{iaw}} \tag{1}$$

where $C_{iw}^{surface}$ is concentration at the water surface. With $\mathcal{M}_{iw} = VC_{iw}^{mean}$, where C_{iw}^{mean} is the mean concentration in the system, we assume that V is constant and divide both sides of Eq. (1) by V and get:

$$\frac{dC_{iw}^{mean}}{dt} = -\frac{A_o}{V} v_{iwa}(C_{iw}^{surface} - C_{iw}^{eq}) = -k_i^{wa}(C_{iw}^{surface} - C_{iw}^{eq}) \quad \text{with} \quad k_i^{wa} = \frac{v_{iwa}}{h}; \quad h = \frac{V}{A_o} \tag{2}$$

where h is the mean depth of the system, k_i^{wa} is the linear rate constant for air–water exchange (dimension T^{-1}). Equation (2) can only be solved if we are able to express the surface concentration in terms of the mean concentration. The "stratification coefficient" is defined as $\sigma = C_{iw}^{surface}/C_{iw}^{mean}$. Then Eq. (2) becomes:

$$\frac{dC_{iw}^{mean}}{dt} = -k_i^{wa}(\sigma C_{iw}^{mean} - C_{iw}^{eq}) \tag{3}$$

If all coefficients in Eq. (3) are constant with time, the solution is (see Eq. 6-8):

$$C_{iw}^{mean}(t) = C_{iw}^{mean\,\infty} + (C_{iw}^{mean\,0} - C_{iw}^{mean\,\infty})e^{-\sigma k_i^{wa} t} \text{ where } C_{iw}^{mean\,\infty} = C_{iw}^{eq}/\sigma \tag{4}$$

$C_{iw}^{mean\,0}$ is initial concentration ($t = 0$) in the system. If the system is completely mixed, the surface and mean concentrations are equal, thus $\sigma = 1$.

19.4 Air–Water Exchange in Flowing Waters

Now we turn our attention to flowing waters. As discussed in Section 19.2, in rivers and streams we expect turbulence induced by friction of the flowing water over the sediment bed to be the dominant source of turbulent energy (see Eq. 19-15). In the following discussion, we focus on the flow-induced contribution to air–water exchange, $v_{iwa}(u_F^*)$. First, in contrast to v_{iw}, the air phase exchange velocity, v_{ia}, is barely affected by the flow. Thus, the following considerations are not relevant for compounds with very small Henry's law coefficients ($K_{iaw} \ll K_{iaw}^{critical} = 10^{-3}$), for which v_{iwa} does not depend on v_{iw}.

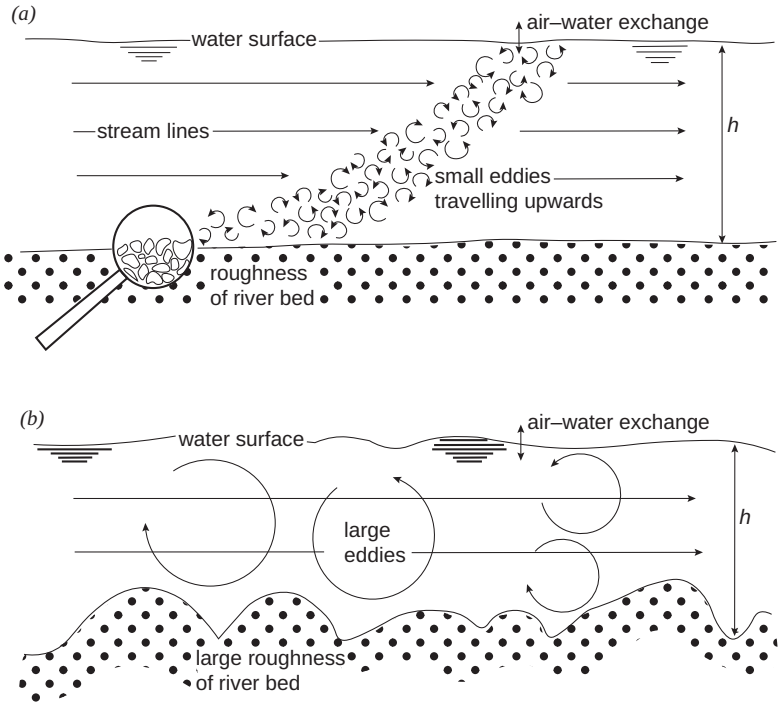

Figure 19.6 Depending on the roughness of a river, stream, or estuary sediment bed, the production of turbulence leads either to (*a*) eddies which are much smaller than the river depth h or to (*b*) large eddies which are able to transport dissolved chemicals fast from and to the water surface. Both situations can be described by different models for air–water exchange: (*a*) the small-eddy model by Lamont and Scott (1970) and (*b*) the large-eddy model by O'Connor and Dobbins (1958).

We introduce here two models that differ in the size of the turbulent eddies relative to the depth of a river or estuary (Fig. 19.6). The eddy size is determined by the flow velocity and by the "topography" of the sediment bed, called the *roughness*. A sediment bed made of sand or silt has a much smaller roughness than a bed made of cobblestones or boulders. The roughness is quantified by the equivalent grain diameter, d_s, the typical diameter of particles forming the bed (Table 19.2). The nondimensional roughness parameter, d^*, then determines the transition between the two eddy size regimes. The small-eddy model applies if (Lamont and Scott, 1970):

$$d^* \equiv \frac{d_s u_F^*}{\nu_w} < 136 \tag{19-21}$$

where ν_w is kinematic viscosity of water (Appendix B.3, Table B.3*a*). The friction velocity, u_F^*, a measure for the average turbulent energy induced by the friction at the river bed, is related to the mean flow velocity of the river, $\bar{u}_F$:

$$u_F^* = \frac{\bar{u}_F}{\alpha} \tag{19-22}$$

where α is a nondimensional factor that typically lies between 10 (rough river bed) and 20 (smooth river bed).

Table 19.2 Equivalent Grain Diameter for Different Sediment Bed Materials

Particle	Typical Diameter, d_s (m)
clay	$<4 \times 10^{-6}$
silt	4×10^{-6} to 1×10^{-4}
sand	1×10^{-4} to 2×10^{-3}
pebble	2×10^{-3} to 0.1
cobble	0.1 to 0.3
boulder	>0.3

Small-Eddy and Small Roughness Model

Qualitatively, a river or estuary with *small roughness* can be visualized as a waterbody in which the turbulent eddies produced by the water currents flowing over the uneven bottom of the sediment bed are much smaller than the depth of the water (Fig. 19.6*a*). When these eddies travel upward from the bottom, they transport turbulent energy to the water surface and thus influence the air–water exchange, modeled by Lamont (1970), Chu and Jirka (2003), and Moog and Jirka (1999a):

$$v_{iw}(u_F^*) = 0.17\,(Sc_{iw})^{-1/2}\left(\frac{\nu_w (u_F^*)^3}{h}\right)^{1/4} = 0.17\,(Sc_{iw})^{-1/2}\left(\frac{\nu_w (\bar{u}_F/\alpha)^3}{h}\right)^{1/4} \tag{19-23}$$

where h is total water depth and Sc_{iw} is the Schmidt number for chemical i in water. Eq. 19-23 is derived so as to arrive at a dimensionally correct expression; hence, the factor 0.17 is independent of a specific choice of units for the involved parameters provided that the used units are consistent. The exponent used for the Schmidt number ($n = -1/2$) has been assumed and is not the result of fitting the model to observations.

From Eq. 19-23, two conclusions can be drawn. First, v_{iw} increases with turbulence intensity (quantified by u_F^*). Also, the influence of a given turbulence intensity on v_{iw} increases with decreasing water depth, h.

In order to compare the flow-induced exchange velocity, $v_{iw}(u_F^*)$, with the wind-induced air–water exchange velocity, $v_{iw}(u_W^*)$, we rewrite Eq. 19-23. For Sc_{iw}, we insert the specific value for the experiments by Chu and Jirka (2003): $i = O_2$, $T = 20°C$ (average), thus $Sc_{O_2w} = 490$ (Appendix B.3, Table B.3*b*), ν_w (20°C) $= 1.00 \times 10^{-6}$ m^2 s^{-1}. The shear velocity, u_F^*, is replaced by the mean river velocity, $\bar{u}_F$, using a medium value $\alpha = 15$ (Eq. 19-22). Since the resulting equation is no longer independent of the specific choice of units, we choose cm s^{-1} for the exchange velocity (as for wind), m s^{-1} for the flow velocity, $\bar{u}_F$, and m for water column depth, h:

$$v_{iw}(\bar{u}_F)(\text{cm s}^{-1}) = 3.26 \times 10^{-3}\left(\frac{[\bar{u}_F(\text{m s}^{-1})]^3}{h(\text{m})}\right)^{1/4} \quad \text{for } Sc_{iw} = 490, T = 20°C \tag{19-24}$$

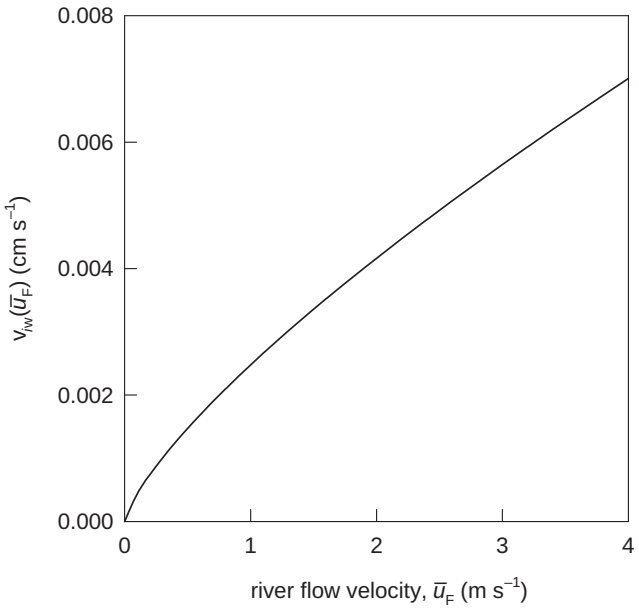

Figure 19.7 Air–water exchange velocity due to river flow, $v_{iw}(\bar{u}_F)$ in cm s^{-1}, as a function of average river flow velocity, $\bar{u}_F$, calculated from Eq. 19-24 for river depth $h = 3$ m and Schmidt number $Sc_{iw} = 490$.

The air–water exchange velocity as a function of mean flow velocity is shown in Fig. 19.7 for $h = 3$ m. By comparing Eq. 19-24 and the air–water exchange velocity due to wind (e.g. Eq. 19-21), we can calculate, for a given river flow velocity, the critical wind velocity above which the contribution from the wind exceeds the contribution from the flow. An example is given in Fig. 19.8. For example, in a river with mean depth of 3 m and $\bar{u}_F = 2.7$ m s^{-1}, wind speed has to become larger than about 10 m s^{-1} in order to become the major factor influencing air–water exchange. At smaller wind speeds, air–water exchange is dominated by the flow-induced shear turbulence.

Large-Eddy Model: Rough River and Estuary Flow

As the roughness of a river, stream, or estuary sediment bed increases, the eddies induced by the irregularities become larger until they extend over the whole waterbody (Fig. 19.7*b*). These macro-eddies allow water to be transported from the bottom to the water surface within short times, thus enhancing the exchange between air and water. According to Moog and Jirka (1999b), the size of the exponent in Eq. 19-23 gradually increases from 1/4 to 1/2. Eventually, the air–water exchange velocity is transformed into the large-eddy model of O'Connor and Dobbins (1958):

$$v_{iw}(\bar{u}_F) = \text{constant} \times \left(\frac{D_{iw}\bar{u}_F}{h}\right)^{1/2} \approx \left(\frac{D_{iw}\bar{u}_F}{h}\right)^{1/2} \qquad (19\text{-}25)$$

where D_{iw} is the molecular diffusion coefficient of substance i in water and the constant is about 1. Equation 19-25 is dimensionally correct (i.e., independent of

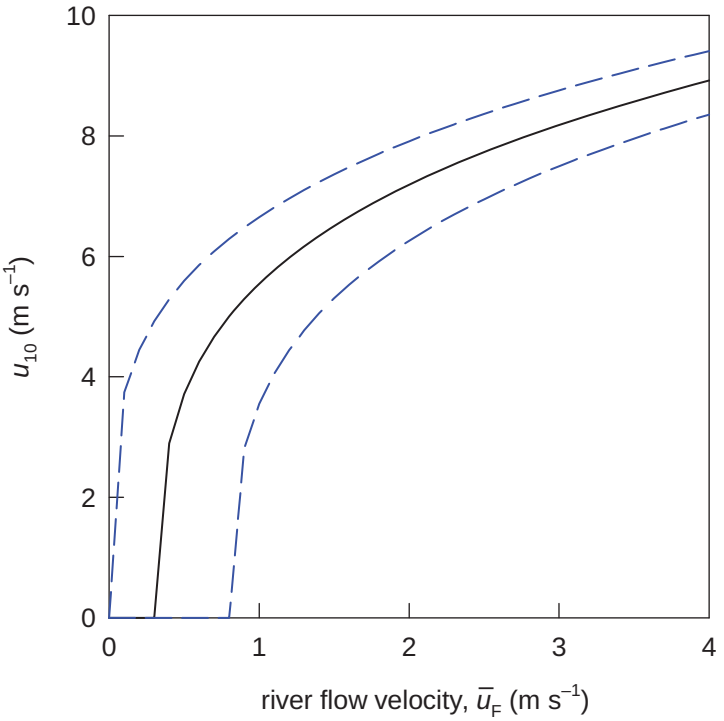

Figure 19.8 Critical wind speed, u_{10}, above which the influence from the wind on air–water exchange, $v_{iw}(u_{10})$, exceeds the influence from river flow, $v_{iw}(\bar{u}_F)$, as a function of average river flow velocity, $\bar{u}_F$. The critical wind speed is calculated by comparing the flow-induced exchange velocity (Eq. 19-24) with Eq. 19-20 with an assumed river depth $h = 3$ m; it does not depend on Schmidt number, since the exponent describing its influence is 1/2 in both equations. Uncertainty of Eq. 19-20 is shown (upper: the constant factor is zero; lower: factor is 18×10^{-4}). For small $\bar{u}_F$, the uncertainty of u_{10} is large. Furthermore, there exists a threshold for $\bar{u}_F$ below which the wind-induced turbulence is always larger than the flow-induced turbulence.

the units) as long as a consistent set of units is used. It can also be written in the form:

$$v_{iw}(\bar{u}_F) = \left(\frac{D_{iw}}{t_{river}}\right)^{1/2}, \text{ with } t_{river} = h/\bar{u}_F \qquad (19\text{-}26)$$

where t_{river} is the transport time over distance h at velocity $\bar{u}_F$. In the light of the surface renewal model, t_{river} adopts the role of the replacement time (Eq. 19-11), except for the factor π. Thus, according to the large-eddy, air–water exchange is controlled by eddies extending over the whole water depth which circle at a speed scaled by the mean current velocity, $\bar{u}_F$.

Enhanced Air–Water Exchange Through Bubbles. If the roughness of the riverbed increases even further, the water surface loses its intact form. Air bubbles are entrained into the water, water droplets are ejected into the air, and foam and spray are formed. The parameter that determines the onset of this kind of enhanced air–water exchange is the nondimensional *element Froude Number*, F_E (see Moog and Jirka, 1999b):

$$F_E = \frac{h\bar{u}_F}{[g(h - h_E)^3]^{1/2}} \qquad h > h_E \qquad (19\text{-}27)$$

where h_E is the typical height of "roughness elements," a length scale which gradually turns into the equivalent grain-size diameter, d_s, if h_E becomes small. Equation 19-27 makes sense only if $h_E < h$, that is, if all "roughness elements" are submerged. For

an alpine stream in which the typical size of the boulders forming the stream bed is larger than the water depth, the above relation is not valid. Empirical expressions for air–water exchange with $F_E > 1.4$ are discussed in Moog and Jirka (1999b).

19.5 Questions and Problems

Special note: Problem solutions are available on the book's website. Solutions to problems marked with an asterisk are available for everyone. Unmarked problems have solutions only available to teachers, practitioners, and others with special permission.

Questions

Q 19.1

What is the most important interface between air and water globally in terms of contact area?

Q 19.2

List some processes that cause organic chemicals in the atmosphere and the ocean to not be at equilibrium.

Q 19.3

Explain the difference between Eqs. 19-1*a* and 19-1*b*.

Q 19.4

How does the exchange velocity, v^*_{itot}, depend on K_{iaw} for large Henry's law coefficients?

Q 19.5

Why can the evaporation rate of water be used to determine the size of the air phase exchange velocity, v_{ia}? *Hint:* Which quantity is the equivalent of the nondimensional Henry's law coefficient for water that has to be used in order to answer this question?

Q 19.6

Explain the difference between the film model and the boundary layer model for air–water exchange. *Hint:* A schematic picture like Fig. 19.1 may help more than a thousand words.

Q 19.7

Exchange velocities, v_{iwa}, are temperature dependent. Explain for the three models (film, wall, boundary layer) how temperature dependence is included and point out the differences between the models regarding their temperature dependence.

Q 19.8

Explain why data of water phase air–water exchange velocities and wind velocities gained by field observation do not lead to a unique relationship between these quantities, especially when wind speed is highly variable. What other factors influence air–water exchange?

Q 19.9

Why do we have to specify the height above the water surface at which wind speed is measured when we formulate an expression that relates the air–water exchange velocity to wind speed? *Hint:* Consider the vertical profile of the horizontal wind speed in light of the "law of the wall."

Q 19.10

In the film model of Whitman, the water phase exchange velocity, v_{iw}, is a function of the molecular diffusion coefficient of the chemical, while in Deacon's boundary layer model, v_{iw} depends on the Schmidt Number, Sc_{iw}. Explain the reason for this difference.

Q 19.11

What makes air–water exchange in rivers different than in the ocean or in a lake?

Q 19.12

What kind of implicit assumption is made in Eq. 19-15 that describes the simultaneous influence of wind and river flow on air–water exchange? Are their possible effects that are ignored by such an assumption?

Q 19.13

Explain the influence of the different quantities appearing in Eq. 19-20 on the air–water exchange velocity.

Q 19.14

How would the critical wind speed as a function of current velocity change, if Fig. 19.7 would be drawn for a river depth of 10 m instead of 3 m? A qualitative argument is sufficient.

Q 19.15

Explain how the large-eddy model for air–water exchange in rivers is related to the surface renewal model.

Problems

P 19.1 *What Is the Source of Benzene in the Water of a Pond?*

Part of your job as a consultant to the State Water Authority is to survey the water quality of several ponds located in a recreation area. Among the volatile organic

compounds, your laboratory monitors the concentration of benzene in the water of various ponds. When inspecting the results, you realize that on certain weekends during the summer, the benzene concentration in the surface water of these ponds is up to ten times higher than in the same ponds in the middle of the week or during the winter. For example, in one pond you measure a peak concentration of 1 μg L^{-1}. You wonder whether this elevated benzene concentration is due to air pollution by the heavy car traffic during the summer weekends, or whether the input occurs primarily by leakage of gasoline and oil from the numerous boats cruising on the ponds. You realize that for assessing this question you need to know something about the benzene concentration in the air. Since you have no measurements from the area, you search the literature and find in a review by Field et al. (1992):

Concentrations of benzene in air

Location	Benzene (ppbv)[a]
remote areas	
Brazil	0.5
Pacific	0.5
urban areas	
Hamburg	3.2 (peak: 20)
London	8.8

[a]Parts per billion on a volume base; use ideal gas law to convert the numbers to molar concentrations

benzene

Answer the following questions:

(a) Is the atmosphere a likely source for the elevated benzene concentrations during the summer weekends? Assume a water temperature of 25°C.

(b) Estimate the direction and rate of air–water exchange of benzene for a wind speed $u_{10} = 2$ m s^{-1}. Use an air concentration of 10 ppbv, a concentration in the water of 1 μg L^{-1}, and a water temperature of 25°C.

(c) Assess the situation for a pond located in the center of a big city for a typical winter day. There are no motorboats on the pond. Use the following conditions: air concentration of benzene 10 ppbv, water concentration 0.1 μg L^{-1}, water temperature 5°C, wind speed $u_{10} = 2$ m s^{-1}.

P 19.2 *Evaluating the Direction of Air–Water Exchange*

C_1 and C_2 halocarbons of natural and anthropogenic origin are omnipresent in the atmosphere and ocean. For example, in the 1980s, typical concentrations in the northern hemisphere air and in Arctic seawater of 1,1,1-trichloroethane (also called methyl chloroform, MCF) and tribromomethane (bromoform, BF) were measured by Fogelqvist (1985).

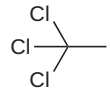

1,1,1-trichloroethane (MCF)

$K_{iH}^{air/seawater}(0°C) = 6.5$ bar L mol^{-1}
$K_{iH}^{air/seawater}(25°C) = 23.8$ bar L mol^{-1}

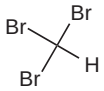

tribromomethane (BF)

$K_{iH}^{air/seawater}(0°C) = 0.20$ bar L mol^{-1}
$K_{iH}^{air/seawater}(25°C) = 0.86$ bar L mol^{-1}

Concentrations of MCF and BF

	MCF (ng L^{-1})	BF (ng L^{-1})
Concentration in air	0.93	0.05
Concentration in Arctic Ocean surface (0-10 m)	2.5	9.8

Using the given concentrations of MCF and BF, evaluate (a) whether there are net fluxes of these compounds between the air and surface waters of the Arctic Ocean assuming water temperatures of 10°C. In each case, if there is a net flux, indicate its direction (i.e., sea-to-air or air-to-sea). Then ascertain whether the rates of air-sea exchange of these halocarbons are (a) air-side controlled, (b) water-side controlled, or (c) both (i.e., at least 10% control by either side) under typical conditions.

Hint: Estimate $K_{iH}^{air/seawater}$ at 10°C from the $K_{iH}^{air/seawater}$ values given for 0°C and 25°C using a temperature dependence of the form (see Eq. 9-26):

$$\ln K_{iH}^{air/seawater}(T) = -\frac{B_i}{T} + A_i$$

where T is the temperature in Kelvin and A_i, B_i are constant parameters that can be determined by the values of $K_{iH}^{air/seawater}$ given for $T = 0°$ and $T = 25°$.

P 19.3* *Evaporation of a Pure Organic Liquid*

Consider a spill of $\mathcal{M}_i = 2$ kg of pure liquid methylchloroform (MCF, molar mass $M_i = 133.4$ g mol^{-1}) forming a puddle on the ground of about $A = 0.3$ m^2 surface area in a closed hall of volume $V = 200$ m^3. Estimate how long it takes for the liquid to completely evaporate at ambient temperatures of 0 and 25°C. Assume that initially the MCF concentration in the air is zero. There is practically no air motion in the hall that could stir the surface of the liquid. The *Handbook of Physics and Chemistry* gives the following saturation vapor pressures of liquid MCF: $p_{iL}^*(0°C) = 4.8$ kPa; $p_{iL}^*(25°C) = 16.5$ kPa.

Hint: As a first approximation, assume that the surface area of the puddle remains constant until all the MCF is evaporated. Also neglect the rising MCF concentration in the hall and check later whether this approximation is justified. If not, refine the calculation. Perhaps a two-box model may help.

P 19.4* *A Lindane Accident in a Drinking Water Reservoir*

Due to an accident, an unknown amount of the insecticide lindane (γ-HCH) is introduced into a well-mixed pond that is used as the drinking water reservoir for a small town. The water inflow and the intake of the waterworks are immediately stopped and the water is analyzed for lindane. In water samples taken at various locations and depths, an average concentration of 5.0 ± 0.2 μg L^{-1} is determined. As a resident of the area, you ask the person in charge of the waterworks what they intend to do about this problem, since 5.0 μg L^{-1} is far above the drinking water limit. "Oh, no problem!" the person tells you, "Within a few days, all lindane will escape into the atmosphere." Being well-trained in environmental organic chemistry, you are very suspicious about

this answer, so you decide to make a calculation. The people from the water works provide you with additional information. With this information and the absolute water vapor pressures listed in Appendix B.3, Table B.3*a*, you can calculate K_{iaw} of water and thus the corresponding air phase exchange velocity, $v_{H_2O\,a}$. Relevant information on lindane can be found in Appendix C.

Pond characteristics

Surface area $A = 5 \times 10^5$ m^2
Volume $V = 2.5 \times 10^6$ m^3
Water temperature $T = 20°$C
Evaporation rate of water at prevailing wind conditions and humidity of 70%:
5 L per m^2 and per day

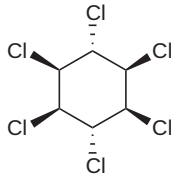

lindane

(a) Calculate the half-life of lindane in the pond (days), assuming that the reservoir volume remains constant. The one-box model introduced in Chapter 6 may help.

(b) Compare the relative loss of lindane from the reservoir to the relative loss of water by evaporation. If the evaporated water were not to be replaced (i.e., no inlets and outlets), would the lindane concentration increase or decrease as a result of the simultaneous water–air fluxes of water and lindane?

P 19.5* *Estimating the Overall Air–Water Exchange Velocity from Wind Speed for Different Water Temperatures*

Calculate the overall air–water exchange velocity, v_{iwa}, of 1,1,1-trichloroethane (methylchloroform, MCF) and tribromomethane (bromoform, BF) at the surface of the ocean for a wind speed of 15 m s^{-1} at seawater temperatures of 25°C and 0°C.

Hint: The necessary information is given in Problem 19.2. Use $D_{H2O\,a} = 0.1$ cm^{2}s^{-1} as molecular diffusivity of water vapor in air at 25°C.

P 19.6* *The Influence of Water Temperature on Air–Water Exchange*

There are several processes that make the air–water exchange velocity, v_{iwa}, temperature-dependent. One results from the temperature dependence of the air–water partition constant, K_{iaw}. If water and air temperatures are different, the question arises whether equilibrium between the air and water phase is determined by water temperature, air temperature, or a mixture of both. Explain why K_{iaw} should be evaluated for the temperature of the water, not the air.

Hint: The process of heat exchange across an interface can be treated in the same way as the exchange of a chemical at the interface. To do so, we must express the molecular thermal heat conductivity by a molecular diffusivity of heat in water and air, $D_{th\,w}$ and $D_{th\,a}$, respectively. At 20° C, we have (see Appendix B.3, Table B.3*a*): $D_{th\,w} = 1.43 \times 10^{-3}$ cm^2 s^{-1}, $D_{th\,a} = 0.216$ cm^2 s^{-1}. Use the film model for air–water exchange with the typical film thicknesses of Eq. 19-9.

P 19.7 *Experimental Determination of the Total Air–Water Exchange Rate for Two Chlorinated Hydrocarbons in a River*

In a field study in the River Glatt in Switzerland, the concentrations of tetrachloroethene (PCE) and 1,4-dichlorobenzene (1,4-DCB) were measured at four

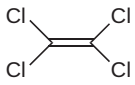

tetrachloroethene

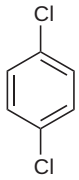

1,4-dichlorobenzene

locations along a river section of 2.4 km length. Any input of water and chemicals can be excluded in this river section. The average depth (h = 0.4 m) and the mean flowing velocity ($\bar{u}_F$ = 0.67 m s^{-1}) were fairly constant in the section. The measurements were made in a way that a specific water parcel was followed downstream and sampled at the appropriate distances. Calculate the mean total air–water exchange velocity, v_{iwa}, of the two substances by assuming that exchange to the atmosphere is the only elimination process from the water and the atmospheric concentration of PCE and 1,4-DCB are very small.

Concentrations of PCE and 1,4-DCB in River Glatt[a]

Distance (m)	PCE (ng L^{-1})	1,4-DCB (ng L^{-1})
0	690 ± 40	234 ± 5
600	585 ± 30	201 ± 5
1200	505 ± 6	180 ± 8
2400	365 ± 10	130 ± 5

[a]Data from Schwarzenbach (1983).

P 19.8* *Air–Water Exchange of Benzene in a River*

benzene

M_i = 78.1 g mol^{-1}
K_{iaw} (25°) = 0.23
$D_{iw} = 1.44 \times 10^{-5}$ cm^2 s^{-1}

You analyze air–water exchange of benzene along a river which consists of three stretches of different bed roughness. The characteristics of the river sections are given in the following table.

River characteristics

Stretch	$\bar{u}$ (m s^{-1})	α (Eq. 19-22)	h (m)	d_s or h_E (m)
A	1	20	1	10^{-3}
B	1	10	1	0.1
C	1	5	1	0.8

Calculate the air–water exchange velocity of benzene at 25°C due to the flow-induced turbulence for the stretches A, B, and C. Compare the result with the wind-induced exchange velocity, v_{iw}, produced by a wind speed u_{10} = 3 m s^{-1}.

P 19.9 *An Inadvertant Air–water Exchange Experiment*

You have worked hard to study the internal dynamics of tetrachloroethene (PCE) and to calculate vertical turbulent diffusion coefficients in lakes. A friend of yours is more interested in the process of air–water exchange. One day, she sees some of your PCE data lying on your desk. She immediately calculates the average v_{iwa} value for the period between June 10 and July 10. You ask her how she gets the result, but she just tells you that she needs to assume that input and output of PCE can be neglected. In addition, for simplicity she assumes that the cross section of the lake, $A(z)$, is independent of depth z, that is, that the lake has the form of a swimming pool with vertical walls. What air–water exchange velocity v_{iwa} does she get?

PCE concentration at depth in a lake

	PCE concentration (10^{-9} mol L^{-1})	
Depth z (m)	June 10	July 10
0	1.0	0.5
2	5.0	2.0
4	9.5	3.5
6	5.5	5.5
8	3.9	4.7
10	3.1	3.6
12	2.6	3.0
14	2.3	2.7
16	2.1	2.4
18	2.0	2.2
20 (bottom)	1.9	2.1

P 19.10* *Air–Water Exchange of Nitrophenols*

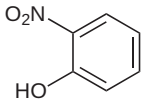

2-nitrophenol

$M_i = 139.1$ g mol^{-1}
p$K_a = 7.15$
$K_{iaw} = 7.9 \times 10^{-4}$

Phenols are organic acids; their dissociation in water is very fast, that is, for most processes we can consider the acid–base equilibrium as an instantaneous equilibrium. The question arises whether the dissociation influences the air–water exchange velocity, and if yes, under which conditions. Before going into much detail, you try to get a first approximate answer based on the information that you have at hand for the two compounds, 2-nitrophenol and 4-nitrophenol. Specifically, you want to answer the question whether for these two substances air–water exchange is affected by dissociation at pH = 7. Use $u_{10} = 1$ m s^{-1} and the usual approximations for the molecular diffusivities. Would your answer be modified for pH = 9.5?

P 19.11 *Air–Water Exchange in an Estuary*

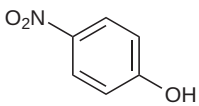

4-nitrophenol

$M_i = 139.1$ g mol^{-1}
p$K_{ia} = 7.06$
$K_{iaw} = 2.2 \times 10^{-8}$

In shallow estuaries that are strongly influenced by tidal currents, air–water exchange can be described by the large-eddy model that was developed for rivers (Eq. 19-26). Assume an average tidal current velocity of 1 m s^{-1} and a water depth of 3 m. For a substance like CO_2, estimate the wind velocity that would cause a similar air–water exchange velocity as the tidal currents.

P 19.12 *PCE in an Evaporative Lake*

In the course of a monitoring program in an evaporative lake with fairly constant volume (lake without outlet in which the inflowing water is balanced by evaporation), a concentration of tetrachloroethene (PCE) of $C_{PCEw}^{mean\,0} = 2.5 \times 10^{-6}$ mol m^{-3} was measured. Earlier measurements had never shown any PCE in the lake. The PCE seemed to be completely mixed in the waterbody. One week later, the concentration had dropped to 1.5×10^{-6} mol m^{-3}. Characteristic lake data are given as follows.

Lake characteristics

Lake volume: $V = 8 \times 10^6$ m^3
Surface area of lake: $A = 1 \times 10^6$ m^2

(a) Estimate the size of the air–water exchange velocity of PCE, $v_{PCE\ wa}$, by assuming that the PCE concentration in the atmosphere is zero and that after the pollution event no additional PCE had entered the lake. Calculate the time until the mean PCE concentration has dropped to 0.1×10^{-6} mol m^{-3}.

(b) It came as a surprise when water samples taken 2 months later still showed a PCE concentration of 0.4×10^{-6} mol m^{-3}. A week later the same concentration was found. Based on measurements of PCE in the air the atmosphere can be excluded as the source of contamination. Apparently, there must be a steady input of PCE into the lake, P. Estimate the size of P.

(c) Closer inspection of the PCE distribution in the lake showed that the concentration at the water surface is only 80% of the mean concentration. How does this finding affect the calculated P-value?

P 19.13* *Dissolution of Non-Aqueous-Phase Liquid (NAPL) into the Aqueous Phase*

Mass exchange between a non-aqueous-phase liquid (NAPL) such as diesel fuel and water can be studied with the so-called slow stirring method (SSM) shown in the following figure (*a*) (Schluep et al., 2001). The temporal increase of the aqueous concentration of four diesel fuel components (benzene, *m*/*p*-xylene, naphthalene) is shown in the same figure. Relevant physicochemical properties are summarized in the given table. The two isomers *m*- and *p*-xylene exhibit virtually the same properties, and are, therefore, considered together.

benzene

(a) In a first step the NAPL–water interface shall be described as a simple bottleneck boundary which separates two homogeneous mixed systems (NAPL, water). Convince yourself that an exchange velocity $v_{ibl} = 3.2 \times 10^{-4}$ cm s^{-1} for *m*/*p*-xylene explains the measured aqueous concentration change reasonably well. Calculate the corresponding water-side boundary layer thickness dbl and use the result to calculate v_{ibl} for benzene and naphthalene.

(b) Why is it reasonable to assume that the exchange across the NAPL–water interface is indeed controlled by a boundary layer in the water and not in the NAPL?

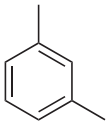

m-xylene

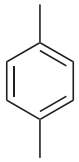

p-xylene

(c) In the SSM setup the water is mixed while the NAPL is not. Modify the model developed in (a) by describing the NAPL as a wall boundary with a water-side boundary layer adjacent to a well-mixed water layer (Fig. 18.6). Is the result very different from (a)?

Hint: Calculate the critical time t_{crit} (Eq 18-32) and compare it to the time scale which is relevant for model (a).

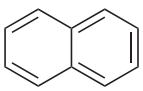

naphthalene

(d) Closer inspection of the temporal change of the aqueous benzene concentration (figure *b*) shows that the steady-state concentration of benzene in the aqueous phase seems to lie about 10% below the equilibrium value with the NAPL phase. Explain the discrepancy.

Physico-chemical Properties of Three Selected Diesel Fuel Compounds (Schluep et al., 2001)[a]

	Benzene	*m/p*-Xylene	Naphthalene
Molar mass M_i (g mol^{-1})	78.1	106.2	128.2
Initial concentration in diesel fuel, $C^{o}_{i\mathrm{NAPL}}$ (mol L^{-1})	9.7×10^{-4}	3.2×10^{-3}	5.5×10^{-3}
Initial mole fraction in NAPL, $x^{o}_{i\mathrm{NAPL}}$ (–)	2.4×10^{-4}	7.9×10^{-4}	1.4×10^{-3}
Liquid aqueous solubility at 20°C, C^{sat}_{iw}(L) (mol L^{-1})	2.2×10^{-2}	1.7×10^{-3}	9.0×10^{-4}
Liquid density at 20°C, ρ_{iL} (g cm^{-3})	0.877	0.873	1.150
Molecular diffusivity in water[b], D_{iw} (cm^2 s^{-1})	9.4×10^{-6}	7.8×10^{-6}	8.2×10^{-6}
Molecular diffusivity in NAPL[b], $D_{i\mathrm{NAPL}}$ (cm^2 s^{-1})	2.2×10^{-6}	1.8×10^{-6}	1.9×10^{-6}

[a]Relevant properties of diesel fuel (NAPL) used for the experiments: molar mass $M_{\mathrm{NAPL}} = 202$ g mol^{-1}; liquid density $\rho_{\mathrm{NAPL}} = 0.8207$ g cm^{-3}; dynamic viscosity at 20°C, η_{NAPL} (20°C) $= 3.64 \times 10^{-2}$ g cm^{-1}s^{-1}.
[b]Approximated from relation by Hayduk and Laudie (1974), see Eq. 17-25; dynamic viscosity of water at 20°C, η_w (20°C) $= 1.002 \times 10^{-2}$ g cm^{-1}s^{-1}.

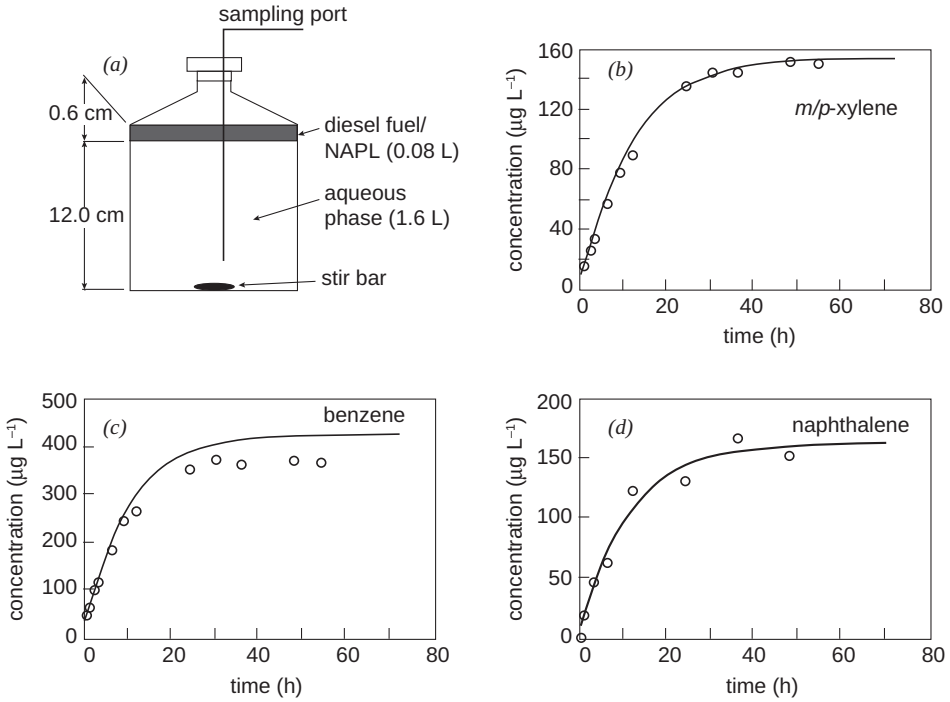

(a) Experimental setup to determine the exchange dynamics of a combined NAPL–water system using the slow stirring method (SSM). (*b*) – (*d*) Measured and calculated aqueous concentrations of benzene; *m/p*-xylene and naphthalene. The solid lines give the result of the linear bottleneck exchange model with an aqueous boundary layer thickness of $\delta_{bl} = 2.4 \times 10^{-2}$ cm = 240 µm. Figure adapted from Schluep et al. (2001).

19.6 Bibliography

Blanchard, D. C.; Woodcock, A. H., Bubble formation and modification in the sea and its meteorological significance. *Tellus* **1957**, *9*, 145–158.

Broecker, W. S.; Peng, T. H., The vertical distribution of radon in the Bomex area. *Earth Planet. Sci. Lett.* **1971**, *11*, 99–108.

Chu, C. R.; Jirka, G. H., Wind and stream flow induced reaeration. *J. Environ. Eng.-ASCE* **2003**, *129*(12), 1129–1136.

Dalton, J., Experimental essays on the constitution of mixed gases; on the force of stream or vapor from waters and other liquids, both in a Torricellian vacuum and in air; on evaporation; and on the expansion of gases by heart. *Mem. Proc. Manchester Lit. Phil. Soc.* **1802**, *5*, 535–602.

Danckwerts, P. V., Significance of liquid–film coefficients in gas absorption. *Ind. Eng. Chem.* **1951**, *43*, 1460–1467.

Deacon, E. L., Gas transfer to and across an air-water interface. *Tellus* **1977**, *29*(4), 363–374.

Emerson, S.; Broecker, W. S.; Schindler, D. W., Gas exchange rate in a small lake as determined by the radon method. *J. Fish. Res. Bd. Can.* **1973**, *30*, 1475–1484.

Fairall, C. W.; Bradley, E. F.; Hare, J. E.; Grachev, A. A.; Edson, J. B., Bulk parameterization of air-sea fluxes: Updates and verification for the COARE algorithm. *J. Clim.* **2003**, *16*(4), 571–591.

Fairall, C. W.; Bradley, E. F.; Rogers, D. P.; Edson, J. B.; Young, G. S., Bulk parameterization of air-sea fluxes for Tropical Ocean Global Atmosphere Coupled Ocean Atmosphere Response Experiment. *J. Geophys. Res.-Oceans* **1996**, *101*(C2), 3747–3764.

Fairall, C. W.; Yang, M. X.; Bariteau, L.; Edson, J. B.; Helmig, D.; McGillis, W.; Pezoa, S.; Hare, J. E.; Huebert, B.; Blomquist, B., Implementation of the Coupled Ocean-Atmosphere Response Experiment flux algorithm with CO_2, dimethyl sulfide, and O_3. *J. Geophys. Res.-Oceans* **2011**, *116*, DOI:10.1029/2010jc006884.

Field, R. A.; Goldstone, M. E.; Lester, J. N.; Perry, R., The sources and behaviour of tropospheric anthropogenic volatile hydrocarbons. *Atmos. Environ.* **1992**, *26A*, 2983–2996.

Fogelqvist, E., Carbon tetrachloride, tetrachloroethylene, 1,1,1-trichloroethane and bromoform in arctic seawater. *J. Geophys. Res.-Oceans* **1985**, *90*(C5), 9181–9183.

Han, P.; Bartels, D. M., Temperature dependence of oxygen diffusion in H_2O and D_2O. *J. Phys. Chem.* **1996**, *100*(13), 5597–5602.

Hayduk, W.; Laudie, H., Prediction of diffusion coefficients for non-electrolytes in dilute aqueous solutions. *Aiche J.* **1974**, *20*, 611–615.

Higbie, R., The rate of adsorption of a pure gas into a still liquid during short periods of exposure. *Trans. Am. Ins. Chem. Eng.* **1935**, *35*, 365–389.

Himmelblau, D. M., Diffusion of dissolved gases in liquids. *Chem. Rev.* **1964**, *64*(5), 527–550.

Jähne, B.; Heinz, G.; Dietrich, W., Measurement of the diffusion coefficients of sparingly soluble gases in water. *J. Geophys. Res.-Oceans* **1987a**, *92*(C10), 10767–10776.

Jähne, B.; Münnich, K. O.; Bösinger, R.; Dutzi, A.; Huber, W.; Libner, P., On the parameters influencing air-water gas exchange. *J. Geophys. Res.-Oceans* **1987b**, *92*(C2), 1937–1949.

Jeffery, C. D.; Robinson, I. S.; Woolf, D. K., Tuning a physically-based model of the air-sea gas transfer velocity. *Ocean Model.* **2010**, *31*(1-2), 28–35.

Johnson, B. D.; Cooke, R. C., Bubble populations and spectra in coastal waters: A photographic approach. *J. Geophys. Res.-Oc. Atm.* **1979**, *84*(C7), 3761–3766.

Johnson, M. T., A numerical scheme to calculate temperature and salinity dependent air-water transfer velocities for any gas. *Ocean Sci.* **2010**, *6*(4), 913–932.

Kanwisher, J., On the exchange of gasses between the atmosphere and the sea. *Deep-Sea Res.* **1963**, *10*, 195–207.

Kolovayev, P. A., Investigation of the concentration and statistical size distribution of wind-produced bubbles in the near-surface ocean layer. *Oceanology* **1975**, *15*(6), 659–661.

Lamont, J. C.; Scott, D. S., An eddy cell model of mass transfer into the surface of a turbulent liquid. *Aiche J.* **1970**, *16*(4), 513–519.

Ledwell, J. J., The variation of the gas transfer coefficient with molecular diffusity. In *Gas Transfer at Water Surfaces*, Brutsaert, W.; Jirka, G., Eds. Springer Netherlands: 1984; Vol. 2, pp 293–302.

Lewis, W. K., The principles of counter-current extraction. *Ind. Eng. Chem.* **1916**, *8*, 825–833.

Lewis, W. K.; Whitman, W. G., Principles of gas absorption. *Ind. Eng. Chem.* **1924**, *16* (1215–1220).

Liss, P. S., Processes of gas exchange across an air–water interface. *Deep Sea Res.* **1973**, *20*, 221–238.

Liss, P. S.; Merlivat, L., Air-sea gas exchange rates: Introduction and synthesis. In *The Role of Air-Sea Exchange in Geochemical Cycling*, Buat-Ménard, P., Ed. D. Reidel: Dordrecht, 1986; Vol. 185, pp 113–127.

Mackay, D.; van Wesenbeeck, I., Correlation of chemical evaporation rate with vapor pressure. *Environ. Sci. Technol.* **2014**, *48*(17), 10259–10263.

Mackay, D.; Yeun, A. T. K., Mass transfer coefficients correlations for volatilization of organic solutes from water. *Environ. Sci. Technol.* **1983**, *17*, 211–233.

Massman, W. J., A review of the molecular diffusivities of H_2O, CO_2, CH_4, CO, O^{-3}, SO_2, NH_3, N_2O, NO, AND NO_2 in air, O^{-2} AND N^{-2} near STP. *Atmos. Environ.* **1998**, *32*(6), 1111–1127.

McGillis, W. R.; Edson, J. B.; Hare, J. E.; Fairall, C. W., Direct covariance air-sea CO2 fluxes. *J. Geophys. Res.-Oceans* **2001**, *106*(C8), 16729–16745.

Monahan, E. C., Oceanic whitecaps. *J. Phys. Oceanogr.* **1971**, *1*, 139–144.

Moog, D. B.; Jirka, G. H., Air-water gas transfer in uniform channel flow. *J. Hydraul. Eng.-ASCE* **1999a**, *125*(1), 3–10.

Moog, D. B.; Jirka, G. H., Stream reaeration in nonuniform flow: Macroroughness enhancement. *J. Hydraul. Eng.-ASCE* **1999b**, *125*(1), 11–16.

Moslashrk, E. T.; Soslashrensen, L. L.; Jensen, B.; Sejr, M. K., Air-sea CO_2 gas transfer velocity in a shallow estuary. *Bound.-Layer Meteorol.* **2014**, *151*(1), 119–138.

Münnich, K. O.; Clarke, W. B.; Fisscher, K. H.; Flothmann, D.; Kromer, B.; Roether, W.; Siegenthaler, U.; Top, Z.; Weiss, W., Gas exchange and evaporation studies in a circular wind tunnel, continuous radon-222 measurements at sea, and tritium/helium-3 measurements in a lake. In *Turbulent Fluxes through the Sea Surface, Wave Dynamics and Predictions*, Favre, H.; Hasselmann, K., Eds. Plenum: New York, **1978**; pp 151–165.

O'Connor, D. J.; Dobbins, W. E., Mechanisms of reaeration in natural streams. *Trans. Am. Soc. Civ. Eng.* **1958**, *123*(1), 641–684.

Oelkers, E. H., Calculation of diffusion coefficients for aqueous organic species at temperatures from 0 to 350°C. *Geochim. Cosmochim. Acta* **1991**, *55*(12), 3515–3529.

Oost, W. A.; Jacobs, C. M. J.; Van Oort, C., Stability effects on heat and moisture fluxes at sea. *Bound.-Layer Meteor.* **2000**, *95*(2), 271–302.

Peng, T.-H.; Broecker, W. S.; Mathieu, G. G.; Li, Y.-H.; Bainbridge, A. E., Radon evasion rates in the Atlantic and Pacific Oceans as determined during the GEOSECS program. *J. Geophys. Res.-Oc. Atm.* **1979**, *84*(C5), 2471–2586.

Penman, H. L., Natural evaporation from open water, bare soil, and grass. *Proc. Roy. Soc. London, Ser. A* **1948**, *193*, 120–146.

Read, J. S.; Hamilton, D. P.; Desai, A. R.; Rose, K. C.; MacIntyre, S.; Lenters, J. D.; Smyth, R. L.; Hanson, P. C.; Cole, J. J.; Staehr, P. A.; Rusak, J. A.; Pierson, D. C.; Brookes, J. D.; Laas, A.; Wu, C. H., Lake-size dependency of wind shear and convection as controls on gas exchange. *Geophys. Res. Lett.* **2012**, *39*, DOI:10.1029/2012gl051886.

Rohwer, E., *Evaporation from free water surfaces*; U.S. Department of Agriculture, 1931.

Satoh, J., Ninjin-island.jpg. Wikicommons: 2008. https://commons.wikimedia.org/wiki/File:Ninjin-island.jpg.

Schluep, M.; Imboden, D. M.; Galli, R.; Zeyer, J., Mechanisms affecting the dissolution of non-aqueous phase liquids into the aqueous phase in slow stirring batch systems. *Environ. Toxicol. Chem.* **2001**, *20*(3), 459–466.

Schwarzenbach, R. P.; Giger, W.; Hoehn, E.; Schneider, J. K., Behavior of organic compounds during infiltration of river water to ground-water. Field studies. *Environ. Sci. Technol.* **1983**, *17*(8), 472–479.

Smith, S. D.; Jones, E. P., Evidence for wind-pumping of air–sea gas exchange based on direct measurements of CO_2 fluxes. *J. Geophys. Res.-Oceans* **1985**, *90*(C1), 869–875.

Stanley, R. H. R.; Jenkins, W. J.; Lott, D. E.; Doney, S. C., Noble gas constraints on air-sea gas exchange and bubble fluxes. *J. Geophys. Res.-Oceans* **2009**, *114*, DOI:10.1029/2009jc005396.

Stevens, B.; Bony, S., Water in the atmosphere. *Phys. Today* **2013**, *66*(6), 29–34.

Sverdrup, H. U.; Johnson, M. W.; Fleming, R. H., *The Oceans: Their Physics, Chemistry, and General Biology*. Prentice-Hall, Inc.: New York, 1942; p 1087.

Torgersen, T.; Mathieu, G.; Hesslein, R. H.; Broecker, W. S., Gas exchange dependency on diffusion coefficient: Direct 222Rn and 3He comparisons in a small lake. *J. Geophys. Res.-Oc. Atm.* **1982**, *87*(C1), 546–556.

Vachon, D.; Prairie, Y. T., The ecosystem size and shape dependence of gas transfer velocity versus wind speed relationships in lakes. *Can. J. Fish. Aquat. Sci.* **2013**, *70*(12), 1757–1764.

Wanninkhof, R., Relationship between wind speed and gas exchange over the ocean. *J. Geophys. Res.-Oceans* **1992**, *97*(C5), 7373–7382.

Wanninkhof, R.; Ledwell, J. R.; Broecker, W. S.; Hamilton, M., Gas exchange on Mono Lake and Crowley Lake, California. *J. Geophys. Res.-Oceans* **1987**, *92*(C13), 14567–14580.